Continental underthrusting and obduction during the Cretaceous closure of the Rocas Verdes rift basin, Cordillera Darwin, Patagonian Andes

Keith Klepeis,[1] Paul Betka,[1,2] Geoffrey Clarke,[3] Mark Fanning,[4] Francisco Hervé,[5] Lisandro Rojas,[6] Constantino Mpodozis,[6,7] and Stuart Thomson[8,9]

Received 8 September 2009; revised 31 January 2010; accepted 12 February 2010; published 29 June 2010.

[1] The Patagonian Andes record a period of Cretaceous-Neogene orogenesis that began with the compressional inversion of a Late Jurassic rift called the Rocas Verdes basin. Detrital zircon ages from sediment that filled the southern part of the basin provide a maximum depositional age of ~148 Ma, suggesting that the basin opened approximately simultaneously along its length during the Late Jurassic. Structural data and U-Pb isotopic ages on zircon from granite plutons near the Beagle Channel (55°S) show that basin inversion involved two stages of shortening separated by tens of millions of years. An initial stage created a small (~60 km wide) thrust wedge that placed the basaltic floor of the Rocas Verdes basin on top of adjacent continental crust prior to ~86 Ma. Structures and metamorphic mineral assemblages preserved in an exhumed middle to lower crustal shear zone in Cordillera Darwin suggest that this obduction was accompanied by south directed subduction of the basaltic crust and underthrusting of continental crust to depths of ~35 km beneath a coeval volcanic arc. A subsequent stage of out-of-sequence thrusting, culminating in the Paleogene, shortened basement and Upper Jurassic igneous rock in the internal part of the belt by at least ~50 km, forming a bivergent thrust wedge. This latter period coincided with the exhumation of rocks in Cordillera Darwin and expansion of the fold-thrust belt into the Magallanes foreland basin. This orogen provides an important example of how orogenesis initiated and led to continental underthrusting and obduction of basaltic crust during closure of a quasi-oceanic rift basin.

Citation: Klepeis, K., P. Betka, G. Clarke, M. Fanning, F. Hervé, L. Rojas, C. Mpodozis, and S. Thomson (2010), Continental underthrusting and obduction during the Cretaceous closure of the Rocas Verdes rift basin, Cordillera Darwin, Patagonian Andes, *Tectonics*, *29*, TC3014, doi:10.1029/2009TC002610.

1. Introduction

[2] In this paper, we present the results of a structural and U-Pb isotopic study of a Cretaceous-Neogene orogen in Patagonia that initiated with the compressional inversion of a Jurassic rift basin [*Dalziel*, 1981; *Wilson*, 1991; *Fildani and Hessler*, 2005; *Calderón et al.*, 2007]. This rift, called the Rocas Verdes basin, is unusual in the Andes because it is the only one of a series of middle to late Jurassic extensional basins south of Ecuador that was floored by basaltic crust with mid-ocean ridge affinities [*Dalziel et al.*, 1974; *Allen*, 1982; *Stern*, 1980; *Alabaster and Storey*, 1990; *Mpodozis and Allmendinger*, 1993; *Calderón et al.*, 2007]. Remnants of this transitional oceanic crust now form a discontinuous belt between the Patagonian batholith, to the south, and the Magallanes foreland basin, to the north (Figure 1). Here, we report on the structure, timing, and mechanisms of basin inversion, including obduction of the quasi-oceanic floor of the Rocas Verdes basin (Figure 1), using exposures in Cordillera Darwin and the western Beagle Channel (55°S).

[3] The northwest arm of the Beagle Channel (Figure 2) is an important locality for understanding the early evolution of the Patagonian Andes because it includes exposures of both the Rocas Verdes mafic crust and a narrow belt of moderate high pressure (7–11 kbar) metamorphic rocks [*Darwin*, 1846; *Nelson et al.*, 1980; *Kohn et al.*, 1993]. These upper amphibolite facies rocks occur exclusively north of the Beagle Channel in Cordillera Darwin. We test the hypothesis that the metamorphic rocks, and structures preserved within them, record the south directed subduction (present coordinates) of the basaltic floor of the Rocas Verdes basin and adjacent continental crust beneath an early Andean arc active during basin closure [*Dalziel*, 1981; *Cunningham*, 1995; *Kraemer*, 2003]. Testing this hypothesis is important because similar mechanisms involving continental underthrusting have been proposed to explain how crustal shortening and uplift are accommodated in other orogens, including beneath Tibet [*Tilmann et al.*,

[1]Department of Geology, University of Vermont, Burlington, Vermont, USA.
[2]Now at the Jackson School of Geosciences, University of Texas at Austin, Austin, Texas, USA.
[3]School of Geosciences, University of Sydney, Sydney, New South Wales, Australia.
[4]Research School of Earth Sciences, Australian National University, Canberra, ACT, Australia.
[5]Departamento de Geología, Universidad de Chile, Santiago, Chile.
[6]Enap-Sipetrol, Santiago, Chile.
[7]Now at Antofagasta Minerals, Santiago, Chile.
[8]Department of Geology and Geophysics, Yale University, New Haven, Connecticut, USA.
[9]Now at the Department of Geosciences, University of Arizona, Tucson, Arizona, USA.

0278-7407/10/2009TC002610

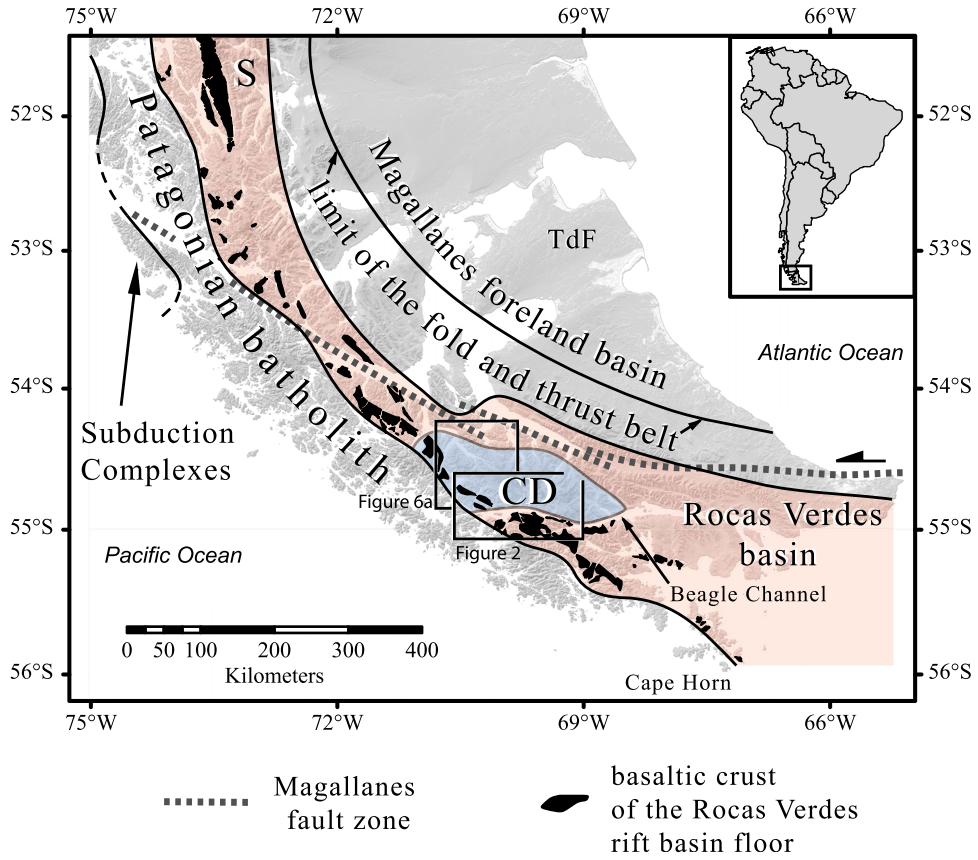

Figure 1. The tectonic provinces of Patagonia. Boxes show locations of Figures 2 and 6a. Shaded relief map incorporates USGS SRTM30 gridded DEM data from the Shuttle Radar Topography Mission. CD, Cordillera Darwin; TdF, Tierra del Fuego; S, Sarmiento complex. Basaltic (quasi-oceanic) rock of the Rocas Verdes terrane is shown in black.

2003], New Zealand [*Stern et al.*, 2002], and the central Andes [*Allmendinger et al.*, 1997; *Beck and Zandt*, 2002; *Sobolev and Babeyko*, 2005]. The Fuegian Andes provide a potentially important example of how this process is influenced by the antecedent geology of a rift basin.

[4] Finally, we determined the structure of Cordillera Darwin and its evolution following obduction of the Rocas Verdes basin floor and collapse of the rift basin. By determining the timing and kinematics of thrust faulting we evaluated potential links between shortening and exhumation in the hinterland, and sedimentation in the adjacent Magallanes foreland basin (Figure 1). This latter goal is important because many previous studies of the Magallanes basin and fold-thrust belt are derived from studies of the provenance and history of foreland sedimentation [e.g., *Wilson*, 1991; *Fildani and Hessler*, 2005; *Barbeau et al.*, 2009; *Romans et al.*, 2010]. Our results show that the structural history we define matches predictions about source areas made by recent analyses of Upper Cretaceous turbidites that filled this basin.

2. Geologic and Tectonic History

2.1. Cordillera Darwin Metamorphic Complex

[5] Cordillera Darwin (CD, Figure 1) forms a topographic high that lies, on average, > 1 km above the surrounding mountains [*Kranck*, 1932; *Nelson et al.*, 1980; *Klepeis*, 1994a; *Kohn et al.*, 1995; *Cunningham*, 1995]. The range has a metamorphic core of pelitic and psammitic schists that forms a topographic culmination within Patagonia

Figure 2. Geologic map of the western Beagle Channel region from this study and data from *Nelson et al.* [1980], *Suárez et al.* [1985] (Isla Gordon), and *Cunningham* [1995] (Bahía Romanche, Caleta Olla, and Roncagli regions). Samples (dots) and U-Pb zircon ages are from this study except GA17B, which is from *Hervé et al.* [2010]. All ages are igneous crystallization ages except 07K21, which is a detrital zircon age. Profiles A-A′, B-B′, C-C′, D-D′, and E-E′ are shown in Figure 3. Ch, Seno Chair (also referred to as Bahía Alemaña); BP, Bahía Pia; BPr, Bahía Parry; BR, Bahía Romanche; CO, Caleta Olla; R, Ventisquero Romanche; SC, Seno Cerrado (also referred to as Bahía España); SG, Seno Garibaldi; SS, Seno Searle; SV, Seno Ventisquero; TB, Bahía Tres Brazos.

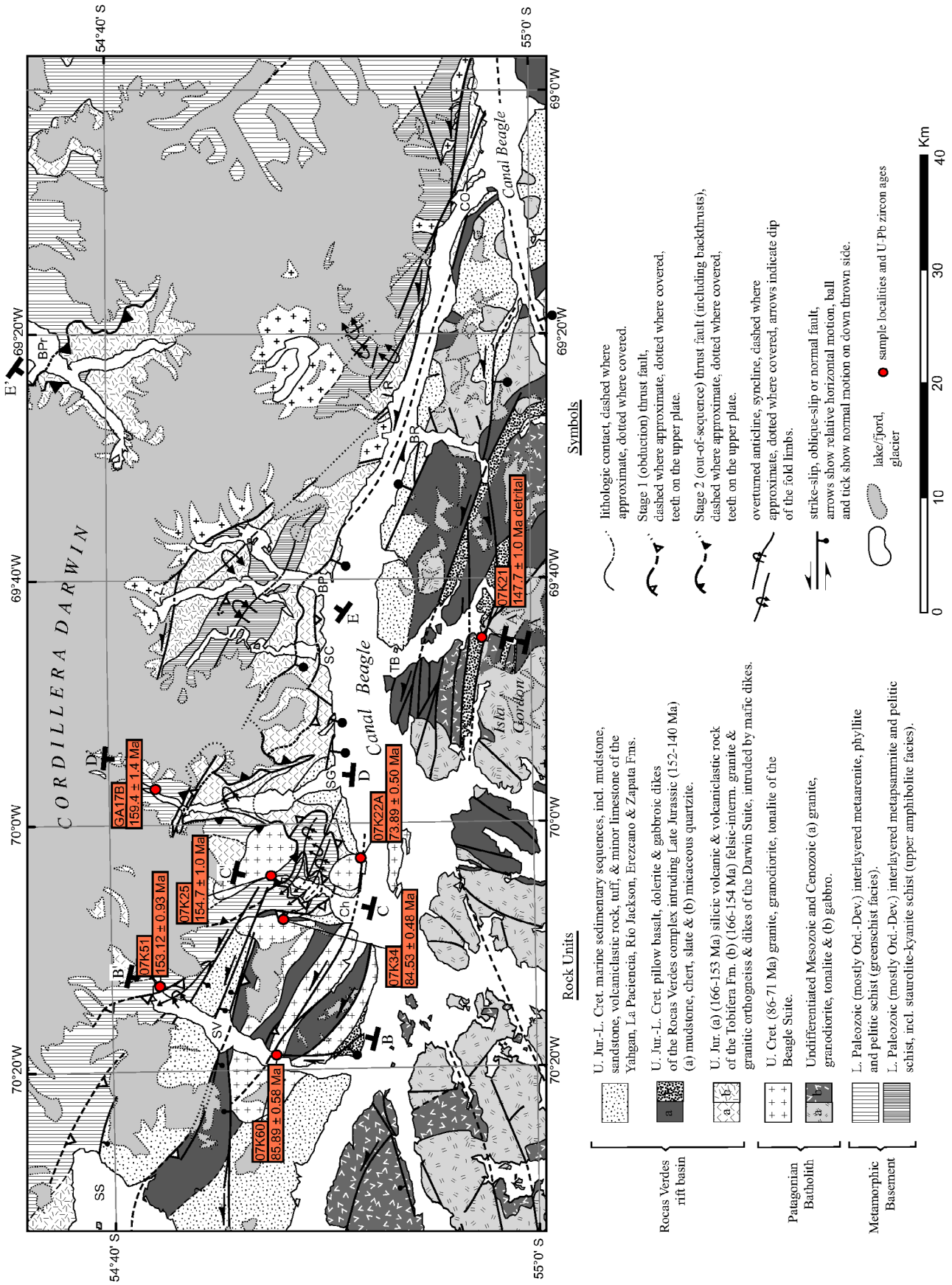
CORDILLERA DARWIN
Canal Beagle
Isla Gordon
70°20'W
70°0'W
69°40'W
69°20'W
54°40' S
55°0' S
07K60 85.89 ± 0.58 Ma
07K51 153.12 ± 0.93 Ma
07K25 154.7 ± 1.0 Ma
GA17B 159.4 ± 1.4 Ma
07K34 84.53 ± 0.48 Ma
07K22A 73.89 ± 0.50 Ma
07K21 147.7 ± 1.0 Ma detrital
Rock Units
Symbols
Rocas Verdes rift basin
Patagonian Batholith
Metamorphic Basement
U. Jur.-L. Cret. marine sedimentary sequences, incl. mudstone, sandstone, volcaniclastic rock, tuff, & minor limestone of the Yahgan, La Paciencia, Río Jackson, Erezcano & Zapata Fms.
U. Jur.-L. Cret. pillow basalt, dolerite & gabbroic dikes of the Rocas Verdes complex intruding Late Jurassic (152-140 Ma) (a) mudstone, chert, slate & (b) micaceous quartzite.
U. Jur. (a) (166-153 Ma) silicic volcanic & volcaniclastic rock of the Tobífera Fm. (b) (166-154 Ma) felsic-interm. granite & granitic orthogneiss & dikes of the Darwin Suite, intruded by mafic dikes.
U. Cret. (86-71 Ma) granite, granodiorite, tonalite of the Beagle Suite.
Undifferentiated Mesozoic and Cenozoic (a) granite, granodiorite, tonalite & (b) gabbro.
L. Paleozoic (mostly Ord.-Dev.) interlayered metaarenite, phyllite and pelitic schist (greenschist facies).
L. Paleozoic (mostly Ord.-Dev.) interlayered metapsammite and pelitic schist, incl. staurolite-kyanite schist (upper amphibolite facies).
lithologic contact, dashed where approximate, dotted where covered.
Stage 1 (obduction) thrust fault, dashed where approximate, dotted where covered, teeth on the upper plate.
Stage 2 (out-of-sequence) thrust fault (including backthrusts), dashed where approximate, dotted where covered, teeth on the upper plate.
overturned anticline, syncline, dashed where approximate, dotted where covered, arrows indicate dip of the fold limbs.
strike-slip, oblique-slip or normal fault, arrows show relative horizontal motion, ball and tick show normal motion on down thrown side.
lake/fjord, glacier
sample localities and U-Pb zircon ages
0 10 20 30 40 Km

Figure 2

(Figure 2). Partially metamorphosed Upper Jurassic and Lower Cretaceous volcanic and sedimentary cover rocks, and Mesozoic-Cenozoic intrusive rocks, surround the metamorphic core [*Dalziel and Elliot*, 1973; *Dalziel*, 1982]. North of the Beagle Channel (Figures 1 and 2), Cretaceous metamorphic mineral assemblages, including garnet, staurolite, kyanite, and sillimanite, occur in basement and cover rocks [*Nelson et al.*, 1980; *Hervé et al.*, 1984; *Kohn et al.*, 1993, 1995]. These upper amphibolite facies assemblages are unique in the Fuegian Andes and record temperatures and pressures of 580°C–600°C and 7–11 kbar, respectively [*Kohn et al.*, 1993]. The basement originally was interpreted as part of a pre-Mid-Jurassic accretionary complex that formed along the western margin of Gondwana [*Kranck*, 1932; *Katz*, 1973; *Dalziel and Elliot*, 1973; *Hervé et al.*, 1981]. However, detrital zircon populations suggest that they differ from metasandstones of the Duque de York Complex (Madre de Diós terrane) outcropping along the westernmost Patagonian archipelagos north of the Magellan Straits [*Hervé et al.*, 2010]. Instead they appear more similar to the Eastern Andes Metamorphic Complex (Fitzroy Terrane of *Hervé and Mpodozis* [2005]), which was deposited on a passive margin and now outcrops along the eastern slope of the Patagonian Andes. Zircon age spectra indicate a mix of sources from different parts of Gondwana, with Ordovician-Devonian [*Hervé et al.*, 2010] and Permian [*Barbeau et al.*, 2009] peaks.

2.2. Late Jurassic Rifting

[6] During the middle to late Jurassic, the Patagonian Andes experienced extension associated with Gondwana breakup [*Bruhn et al.*, 1978; *Dalziel*, 1981; *Pankhurst et al.*, 2000]. The eruption of large volumes of rhyolitic tuffs and the deposition of silicic volcaniclastic sediment of the Upper Jurassic Tobifera Formation accompanied rifting [*Natland et al.*, 1974; *Gust et al.*, 1985; *Hanson and Wilson*, 1991; *Pankhurst et al.*, 2003], which occurred at least from ~152 to ~142 Ma [*Calderón et al.*, 2007]. By the Early Cretaceous, the extension had formed the Rocas Verdes basin, a rift basin floored by quasi-oceanic crust [*Katz*, 1973; *Dalziel et al.*, 1974, *Dalziel*, 1981; *Fildani and Hessler*, 2005; *Calderón et al.*, 2007]. South of 51°S, deformed remnants of the upper part of the Rocas Verdes basin floor now form the Sarmiento and Tortuga ophiolitic complexes (Figure 1) [*Suárez and Pettigrew*, 1976; *Stern*, 1980; *Allen*, 1982; *Wilson*, 1983; *Alabaster and Storey*, 1990; *Calderón et al.*, 2007]. The basin fill includes the shale-dominated Lower Cretaceous Zapata, Yahgan, and La Paciencia formations, which overlie the Tobifera Formation [*Wilson*, 1991; *Dalziel and Elliot*, 1971; *Alvarez-Marrón et al.*, 1993; *Olivero and Martinioni*, 2001; *Olivero and Malumián*, 2008]. These units thicken to the southeast, reflecting a basin that was at least wider and, possibly, deeper in the south [*Katz*, 1963; *Dott et al.*, 1982; *Calderón et al.*, 2007]. *Hervé et al.* [2007] present evidence for the existence of a magmatic arc that rimmed the rift basin north of the Magellan Straits. However, no evidence exists for an active magmatic arc south of Tierra del Fuego until the Late Cretaceous (see discussion by *Mpodozis and Rojas* [2006]).

2.3. Rift Basin Inversion, Collapse, and Formation of the Magallanes Foreland Basin

[7] Cretaceous-Neogene crustal shortening closed the Rocas Verdes basin, formed the Magallanes foreland basin, and created the Magallanes fold-thrust belt (Figure 1). The exact age of the transition from rifting to contraction is poorly known. Deformed fossils indicate that shortening initiated sometime after the Albian-Aptian [*Halpern and Rex*, 1972; *Dott et al.*, 1977]. North of the Magellan Straits (Última Esperanza Region), deposition of the Upper Cretaceous Punta Barrosa Formation has been interpreted to mark the onset of thrusting and sedimentation into the Magallanes foreland basin [*Biddle et al.*, 1986; *Wilson*, 1991; *Fildani and Hessler*, 2005; *Olivero and Malumián*, 2008]. The age of this clastic fill, originally interpreted as late Albian-Aptian to Cenomanian [*Katz*, 1963; *Natland et al.*, 1974; *Wilson*, 1991], was revised to ~92 Ma on the basis of detrital zircon ages [*Fildani et al.*, 2003]. Stratigraphically above this unit are deep-water conglomerates and slope and deltaic systems [*Natland et al.*, 1974; *Biddle et al.*, 1986; *Wilson*, 1991; *Fildani and Hessler*, 2005; *Hubbard et al.*, 2008; *Romans et al.*, 2010].

[8] Coinciding with the development of the flexural Magallanes foreland basin and fold-thrust belt, rocks now exposed in Cordillera Darwin experienced moderate high pressure metamorphism [*Halpern*, 1973; *Nelson et al.*, 1980; *Kohn et al.*, 1995]. *Nelson et al.* [1980] defined three phases of mid-Cretaceous deformation that predated intrusion of late Cretaceous granite plutons of the Beagle suite: an initial phase (D_1) of continent-directed thrusting, inferred to have resulted in the obduction of the Rocas Verdes floor, followed by conjugate back folding (D_2) and a third phase (D_3) of south vergent folding. The first two phases were interpreted to have accompanied burial and high-grade metamorphism. The $^{40}Ar/^{39}Ar$ cooling ages [*Kohn et al.*, 1995] and fission track thermochronology [*Nelson*, 1982] indicate that an initial pulse of cooling (T = 550°C–325°C) and exhumation occurred from ~90 to ~70 Ma. A second pulse of cooling (T < 250°C) and exhumation occurred from the Paleocene to the Middle Eocene [*Kohn et al.*, 1995; *Barbeau et al.*, 2009; *Gombosi et al.*, 2009]. Various mechanisms controlling exhumation have been proposed, including erosion related to thrust faulting [*Klepeis*, 1994a; *Kraemer*, 2003; *Barbeau et al.*, 2009; *Gombosi et al.*, 2009] and transpression [*Cunningham*, 1995] and denudation by normal faulting [*Dalziel and Brown*, 1989; *Kohn et al.*, 1995]. As rocks in Cordillera Darwin were exhumed, thin-skinned thrust sheets propagated into the Magallanes foreland, terminating in the Eocene [*Alvarez-Marrón et al.*, 1993; *Ghiglione and Ramos*, 2005; *Barbeau et al.*, 2009; *Gombosi et al.*, 2009].

2.4. Strike-Slip Faulting

[9] Beginning in the late Oligocene or early Neogene, convergence in the southernmost Andes declined and sinistral strike-slip faulting dominated [*Cunningham*, 1993; *Klepeis*, 1994b; *Klepeis and Austin*, 1997; *Diraison et al.*, 2000; *Ghiglione and Ramos*, 2005; *Lodolo et al.*, 2003; *Gombosi et al.*, 2009]. This transition coincides with for-

mation of the South American-Scotia transform fault boundary [*Rossello*, 2005]. The Magallanes-Fagnano fault, the Carabajal valley and the Beagle Channel fault zone form part of this boundary on Tierra del Fuego (see *Menichetti et al.* [2008] for a review).

3. Structural Geology

[10] We divide the study area (Figure 2) into four domains that are defined by similarities in the style, metamorphic grade and relative ages of structures. These domains are (1) the Rocas Verdes terrane, (2) a zone of obduction structures and crosscutting granite plutons, (3) a zone of back thrusts and back folds, and (4) a domain of high-grade metamorphic rocks and thrust fabrics.

3.1. Rocas Verdes Terrane

[11] Bahía Tres Brazos (TB, Figure 2) exposes arrays of gabbroic dikes that intrude a low-grade metasedimentary sequence of quartzite, greenschist, metasiltstone, and slate. The dikes display igneous mineral assemblages; including hornblende, clinopyroxene and plagioclase; that are partially replaced by chlorite and actinolite. Along a 1 km section, dike spacing ranges from zero (i.e., sheeted dikes) to > 75 m (Figure 3a) and most dikes are steep (Figure 4a). These observations indicate that this locality exposes the sheeted dike and gabbroic part of the Rocas Verdes ophiolite suite described by *Suárez et al.* [1985] and *Cunningham* [1994].

[12] The gabbroic dikes mostly lack a penetrative subsolidus foliation, except along their margins where zones of steeply dipping cleavage defined by aligned chlorite and actinolite locally occur. In contrast, metasedimentary rock that hosts the dikes generally contains a penetrative greenschist facies foliation defined by the alignment of muscovite, chlorite and flattened quartz. In most places, this latter foliation is steep and parallels the axial planes of tight folds of bedding. Some dike margins also are folded. Delicate primary structures, including cross beds, mud-filled burrows and evidence of bioturbation, are present in sedimentary layers. On the basis of the preservation of these delicate structures and the lack of penetrative deformation of the dikes, strain magnitudes appear to be mostly low in this part of the section. The exception is inside narrow (tens of meters thick) strike-slip faults of the Beagle Channel fault zone (section 3.5). The general lack of deformation in most dikes, and their steep orientation regardless of proximity to faults, supports the conclusion of *Cunningham* [1994], who interpreted the steep orientations as a primary feature of the Rocas Verdes basin floor.

3.2. Obduction Structures and Beagle Suite Plutons

[13] Seno Ventisquero (SV, Figure 2) exposes an interlayered sequence of deformed gabbroic dikes, metabasalt, amphibolite and micaceous quartzite that is similar in composition to the sequences in Bahía Tres Brazos. The main difference between these two localities is that the assemblages in Seno Ventisquero are penetratively foliated, folded, titled, and thickened by at least two northeast vergent ductile thrusts (Figures 2, 3b, and 4b). The largest thrust places metabasaltic rock, amphibolite, and metasedimentary rock on top of openly folded, weakly cleaved mudstones of the Lower Cretaceous Yahgan Formation (Figure 3b). At least one other thrust internally thickens the sequence, which is at least 3.75 km thick. The thrusts themselves are defined by zones (at least several tens of meters thick) of sheared quartzite and gabbroic layers that are thinner and more attenuated than those exposed in Bahía Tres Brazos (Figure 4b). Isoclinal, intrafolial folds (F_1) of compositional layering are common. Quartzite layers are mylonitic and display downdip quartz ribbons and muscovite mineral lineations (L_1). In basaltic and amphibolite layers, a penetrative greenschist facies foliation (S_1) dips gently and moderately to the southwest (Figure 4b) and contains a downdip chlorite and actinolite mineral lineation (L_1). Asymmetric structures, including amphibole fish and oblique foliations, record a top-to-the-northeast sense of movement on surfaces oriented parallel to L_1 and perpendicular to S_1.

[14] In northern Seno Ventisquero, one of the lowest thrusts of the stack cuts the basement-cover contact and is folded by southwest vergent back folds (Figures 2 and 3b). This contact is marked by the structurally lowest of a series of granitic dikes of the Upper Jurassic Darwin suite (see also section 4.2) that intrude basement schist. Basement is distinguished from cover rocks on the basis of composition, metamorphic grade, and stratigraphic position below the Upper Jurassic cover rocks. The basement consists of alternating layers of polydeformed metapsammite and muscovite schist that are full of tightly folded quartz veins and superposed cleavages that contrast with the weakly deformed granitic dikes. Lower Cretaceous rocks in this fjord also are easily distinguishable from basement because the former lack muscovite and are dominated by mudstone rather than sandstone. *Hervé et al.* [2010] report detrital zircon ages from the mudstone that confirm an Early Cretaceous depositional age (Figure 3b). The thrust is defined by a zone of recrystallized quartz layers, dikes and veins that displays a penetrative downdip quartz-mica mineral lineations (L_1), and shear bands with asymmetric quartz porphyroclasts. The asymmetric structures record a top-to-the-northeast sense of displacement despite the folding.

[15] These thrusts are important because they represent the first documented series of faults responsible for placing quasi-oceanic rocks of the Rocas Verdes suite onto Lower Cretaceous basin infill and basement rock in southern Cordillera Darwin. This thrusting event marks the obduction of the Rocas Verdes basin basaltic floor onto the South American continent. We traced these thrusts to the east and southeast into adjacent fjords. In Seno Chair (Figure 2), two northeast vergent thrusts place metavolcanic rock of the Tobifera Formation on top of basement pelites of the Darwin metamorphic complex (Figures 2 and 3c). These exposures show that the obduction thrusts cut up section across the basement-Tobifera contact. The northernmost thrust is folded by back folds (Figure 3c, section 3.3). The southernmost thrust trends into Seno Garibaldi (SG, Figure 2) where it is cut by a large south vergent back thrust (Figure 3d, section 3.3). East of Seno Garibaldi this thrust zone occurs within the Tobifera Formation at the mouth of Bahía Pia (Figure 2).

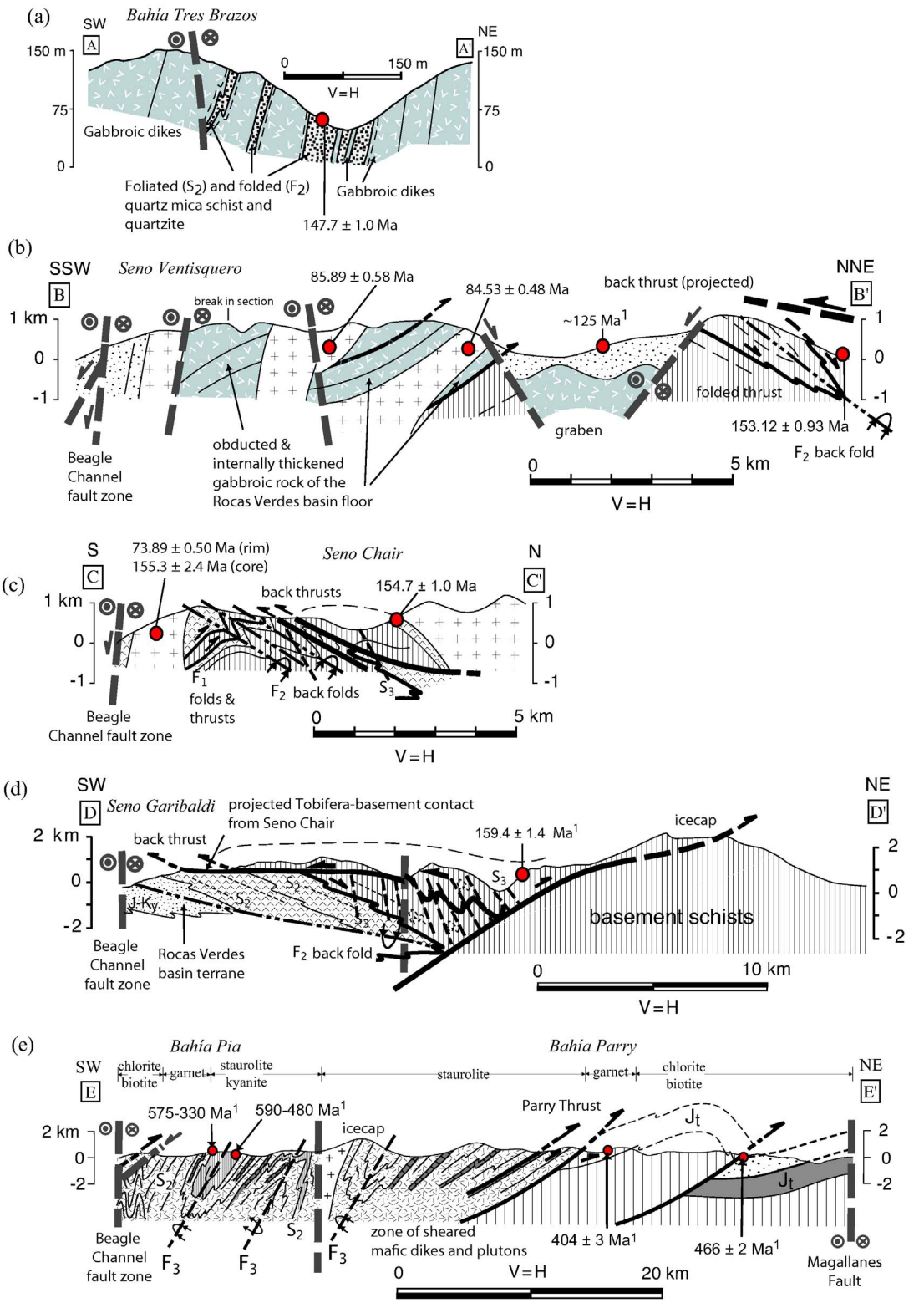

Figure 3. Cross sections of regions south (A-A′) and north (B-B′, C-C′, D-D′, and E-E′) of the Beagle Channel (see Figure 2 for locations). Ages labeled with a superscript 1 are from *Hervé et al.* [2010]. All other ages are reported in this paper. Geologic patterns are same as in Figure 2. J_t, Upper Jurassic Tobifera Formation.

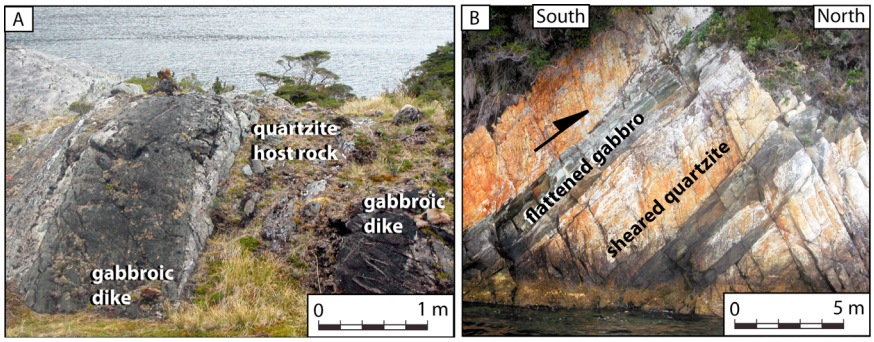

Figure 4. Photographs of (a) weakly deformed, steep gabbroic dikes intruding quartzite host rock at Bahía Tres Brazos and (b) flattened, stretched, and tilted gabbroic dikes intruding sheared quartzite sequence in Seno Ventisquero.

[16] Between Seno Ventisquero and Seno Garibaldi, five granitic plutons of the Beagle suite cut across all fabrics that define the obduction-related thrusts (Figures 2, 3b, and 3c). This crosscutting relationship indicates that the thrusts all occurred prior to the intrusion of the plutons [see also *Nelson et al.*, 1980]. In most areas, the plutons form sheets up to several kilometers thick. Each lacks a penetrative subsolidus fabric except in narrow zones where younger brittle, semibrittle and ductile strike-slip and oblique-normal faults cut them (section 3.5).

3.3. Back Folds and Back Thrusts

[17] At the northern ends of Seno Ventisquero and Bahía Chair (Figure 2), and in central Seno Garibaldi (Figures 3a–3c), a series of south and southwest vergent back folds (F_2) deform older, obduction phase folds (F_1) and fabrics (L_1/S_1). Within these zones, folded L_1 quartz-mica mineral lineations on S_1 thrust surfaces are visible (Figures 5a–5c). Oblique quartz foliations, asymmetric tails on quartz-feldspar aggregates, and shear bands record a top-to-the-northeast sense of shear within the S_1/L_1 thrust fabric despite its reorientation by the back folds (Figures 3b and 5b). The back folds plunge to the northwest by 15°–20° and display a crenulation cleavage (S_2) that dips gently to moderately to the north and northeast and parallels the axial planes of the folds. The largest folds are synclinal, although parasitic fold trains of anticlines and synclines are common (e.g., Figure 3c). The S_2 crenulations commonly form shear bands that record a top-to-the-south sense of shear in zones of subparallel back thrusts (Figures 5d–5f) up to several hundred meters thick (Figure 3c). These structures define a phase of south and southwest vergent deformation that postdates obduction.

[18] In Seno Garibaldi, a large back thrust in basement phyllites shears out the upper limb of an overturned F_2 syncline, first described by *Nelson et al.* [1980] (Figures 2 and 3d) [see also *Álvarez*, 2007]. The syncline folds a sequence of basement, volcaniclastic rock of the Tobifera Formation, and mudstone and siltstone of the Yahgan Formation. As in the fjords to the west (Figures 5a–5c), the back folds deform an older obduction phase thrust (S_1/L_1 fabric) that records top-to-the-northeast displacements. The back thrust, which is well exposed at sea level, is defined by a penetrative crenulation cleavage (S_2) that dips gently to the north and parallels the axial planes of rootless, isoclinal F_2 folds. Quartz rods and stretched quartz-feldspar aggregates define a penetrative downdip stretching lineation (L_2) on cleavage planes. Shear bands record top-to-the-south displacements on surfaces that parallel L_2 and are perpendicular to S_2 (Figure 5d).

[19] Superimposed on the back folds and back thrusts is a 10–15 km wide zone of crenulation cleavage (S_3) that dips variably to the north (Figure 3d) and trends northwest between Seno Garibaldi and Seno Agostini (Figure 6a). The S_3 cleavage [see also *Nelson et al.*, 1980], overprints all S_2 cleavage and parallels the axial planes of F_3 folds. Variations in the orientation and degree of fold tightness allowed us to determine the kinematic significance of the F_3/S_3 structures. In Seno Garibaldi the zone of crenulation cleavages is centered on an exposed back thrust (Figures 3d and 6). Along a continuous transect from several kilometers below (south of) the back thrust to the back thrust itself, we observed the following trends: at the southern edge of the zone of S_3 crenulation cleavage, F_3 folds are upright open chevrons displaying a near vertical axial planar S_3 cleavage (Figure 7a). North and toward the back thrust, the F_3 folds tighten, become asymmetric, and overturn to the south (Figures 7b and 7c). Accompanying this change in fold shape and orientation, the average northerly dip of S_3 cleavage planes shallows by ~36° (Figure 6b) and the pattern of cleavage changes from weak and widely spaced to penetrative. Type 3 [*Ramsey*, 1967] fold interference patterns (Figures 7b, 7c, and 7d) are common, indicating that F_2 and F_3 folds are coaxial (Figures 7e, 7f, and 7g). These patterns define a strain gradient that shows an increase in flattening from below (south of) the back thrust at the edge of the zone of crenulation cleavage toward the center of this zone. The accompanying change in the dip of S_3 cleavage also indicates a sense of rotation to the south and southeast. This sense of rotation is identical to that recorded by the S_2 shear bands that define the back thrusts. We, therefore, interpret this zone of S_3 crenulation cleavages as being kinematically related to top-to-the-south back thrusting.

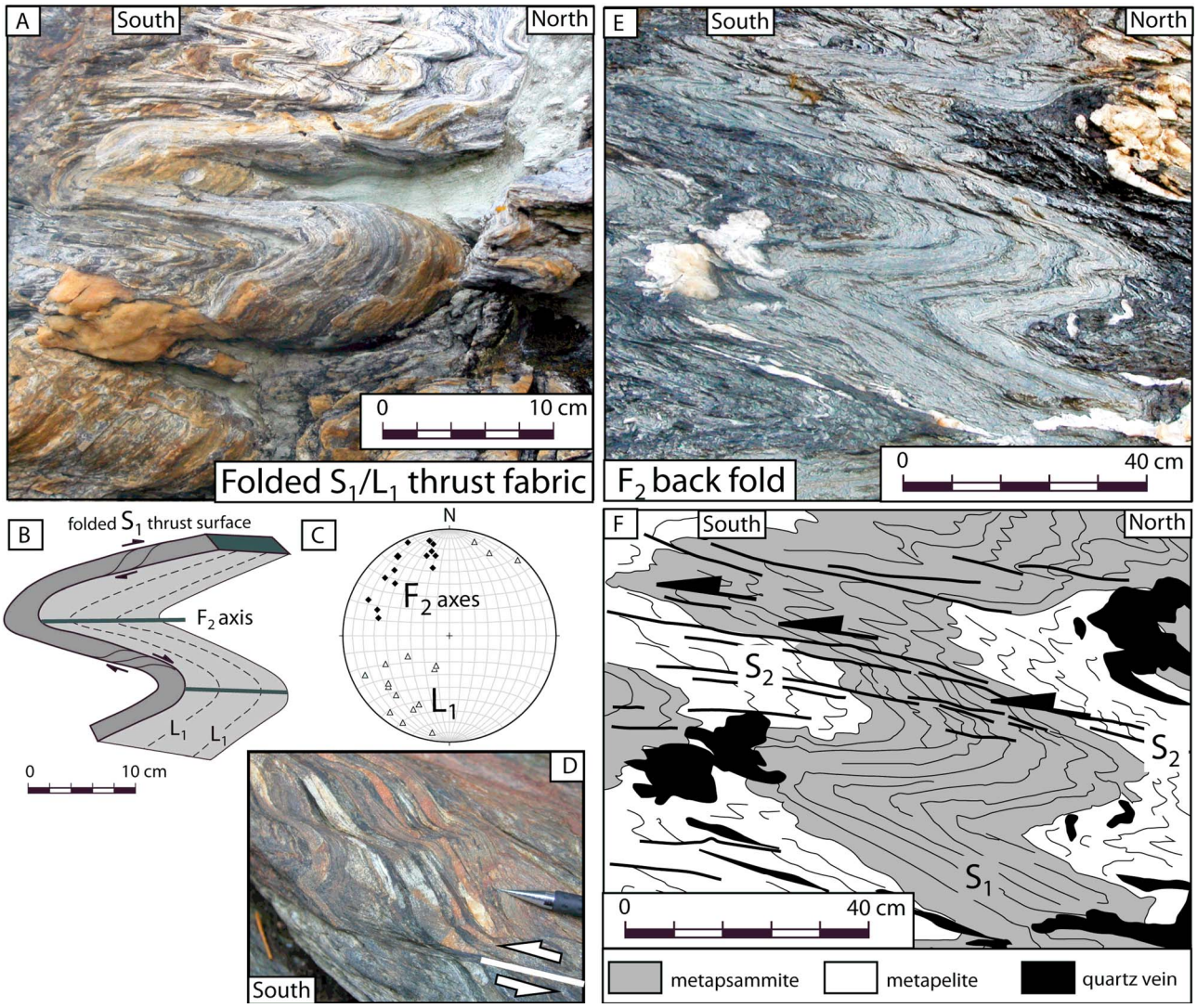

Figure 5. Structural relationships in the domain of back thrusting and back folding, senos Chair and Garibaldi. (a) Photograph and (b) summary sketch of obduction phase thrust fabric (S_1/L_1) in basement phyllites that is folded by south vergent back folds, Seno Chair. (c) Lower hemisphere equal-area stereoplot showing SW and NE plunging L_1 mineral lineations folded by NW plunging F_2 folds. (d) Photograph of shear bands showing a top-to-the-south sense of shear in a back thrust, Seno Garibaldi. (e) Photograph and (f) summary sketch of back folded S_1 cleavage in basement schist, Seno Chair. Back fold is characterized by north dipping asymmetric crenulation cleavages (S_2) and microfaults displaying a top-to-the-south sense of shear.

3.4. Zone of High-Grade Metamorphic Rocks and Thrust Fabrics

[20] The high-grade metamorphic core of Cordillera Darwin occurs between Seno Cerrado in the northwest and Ventisquero Roncagli in the southeast (Figure 2). Within this narrow belt, upper amphibolite facies mineral assemblages in both basement and cover rock (Figure 6b) reflect closure of the Rocas Verdes basin [*Nelson et al.*, 1980; *Kohn et al.*, 1993, 1995].

[21] We report here, for the first time, that a northeast vergent ductile thrust fault forms the northern boundary of the high-grade core in Bahía Parry (Figures 2 and 3e). This fault, the Parry thrust, is defined by penetratively foliated greenschist facies rocks, and dips moderately to the southwest. In the hanging wall, sheared granitic orthogneiss of the Darwin suite intruded staurolite-bearing basement screens. As the fault is approached from south to north, sheared mafic dikes reflect progressively higher strain and become progressively more closely aligned with the Parry thrust (Figure 3e). There is an abrupt decrease in metamorphic grade across the fault (Figure 6b), as the footwall is composed of deformed mafic dikes in greenschist facies basement

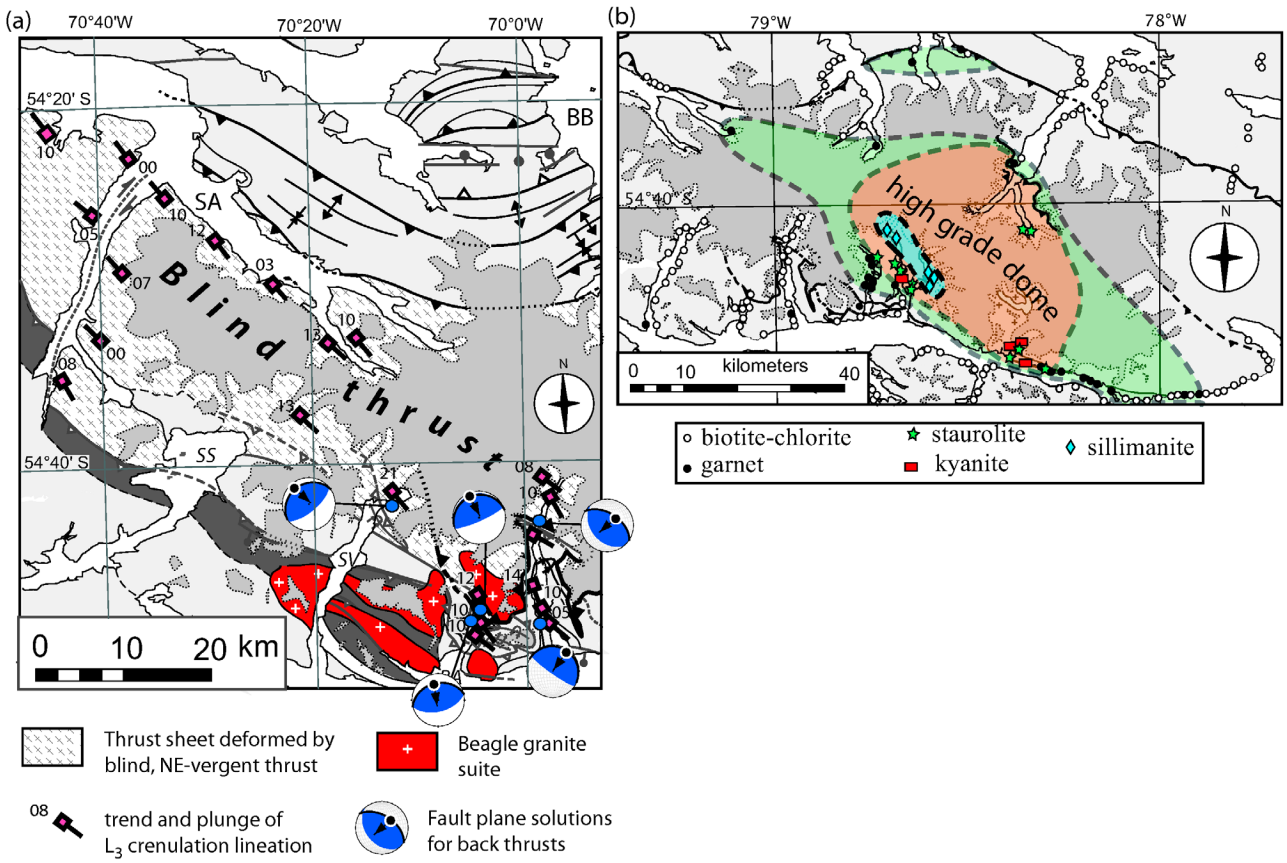

Figure 6. (a) Simplified map (location in Figure 1) of western Cordillera Darwin showing the orientation of L_3 crenulation lineations in the domain of back thrusting and back folding. Lineation data are from this study and from *Nelson et al.* [1980]. The zone of S_3 cleavage marks the location of a blind, northeast vergent thrust that lies between a back thrust in the south and another northeast vergent thrust north of Seno Agostini (SA). Fault plane solutions for back thrusts are shown on lower hemisphere equal-area stereoplots that incorporate data on fault plane orientation (black great circles), mineral striae (black dots), and sense of motion of the hanging wall (arrow). (b) Simplified map of Cordillera Darwin showing the distribution of metamorphic index minerals after *Kohn et al.* [1995], *Ortiz* [2007], and this study. The assemblages define an antiformal dome of high-grade rocks centered on Bahía Pia and bounded on the north by the Parry thrust and on the south by faults at the mouth of Bahía Pia.

phyllites. The thrust includes a penetrative downdip quartz-muscovite mineral lineation. Boudinaged dikes indicate high strains and show that this mineral lineation represents a true stretching lineation. Sense of shear indicators, viewed on surfaces oriented parallel to the mineral lineation and perpendicular to foliation, include C′ shear bands, asymmetric recrystallized tails on feldspar clasts (σ type) and asymmetric muscovite fish. These observations indicate that the high-grade core was displaced to the northeast along the Parry thrust.

[22] At the mouth of Bahía Pia, the southern boundary of the high-grade core is defined by a gently dipping normal fault (first reported by *Dalziel and Brown* [1989]) that forms part of the Beagle Channel fault zone (section 3.5). This normal fault constitutes part of a ~10 km wide extensional step over between sinistral strike-slip fault arrays. The normal fault cuts foliations that reflect the obduction phase (thrusting) in low-grade (greenschist facies) rocks of the Tobifera Formation, which form the hanging wall. The footwall is composed of orthogneiss and high-grade schist. The contrast in metamorphic grade across this normal fault shows that transtensional faults of the Beagle Channel fault zone control the metamorphic break between high-grade rocks (to the north) and low-grade rocks (to the south of the channel).

[23] Within the high-grade core at Bahía Pia and Ventisquero Roncagli, four rock units have been defined [see also *Álvarez*, 2007]. Paleozoic basement includes interlayered metapelitic schist and metapsammite, graphitic schist, and metavolcaniclastic rocks. Granitic dikes and sills of the Late Jurassic Darwin suite intruded these basement rocks. In most places, these dikes and sills form thick sheets and lenses of orthogneiss interfolded with the basement schists. Swarms of mafic (amphibolite) dikes that intrude the

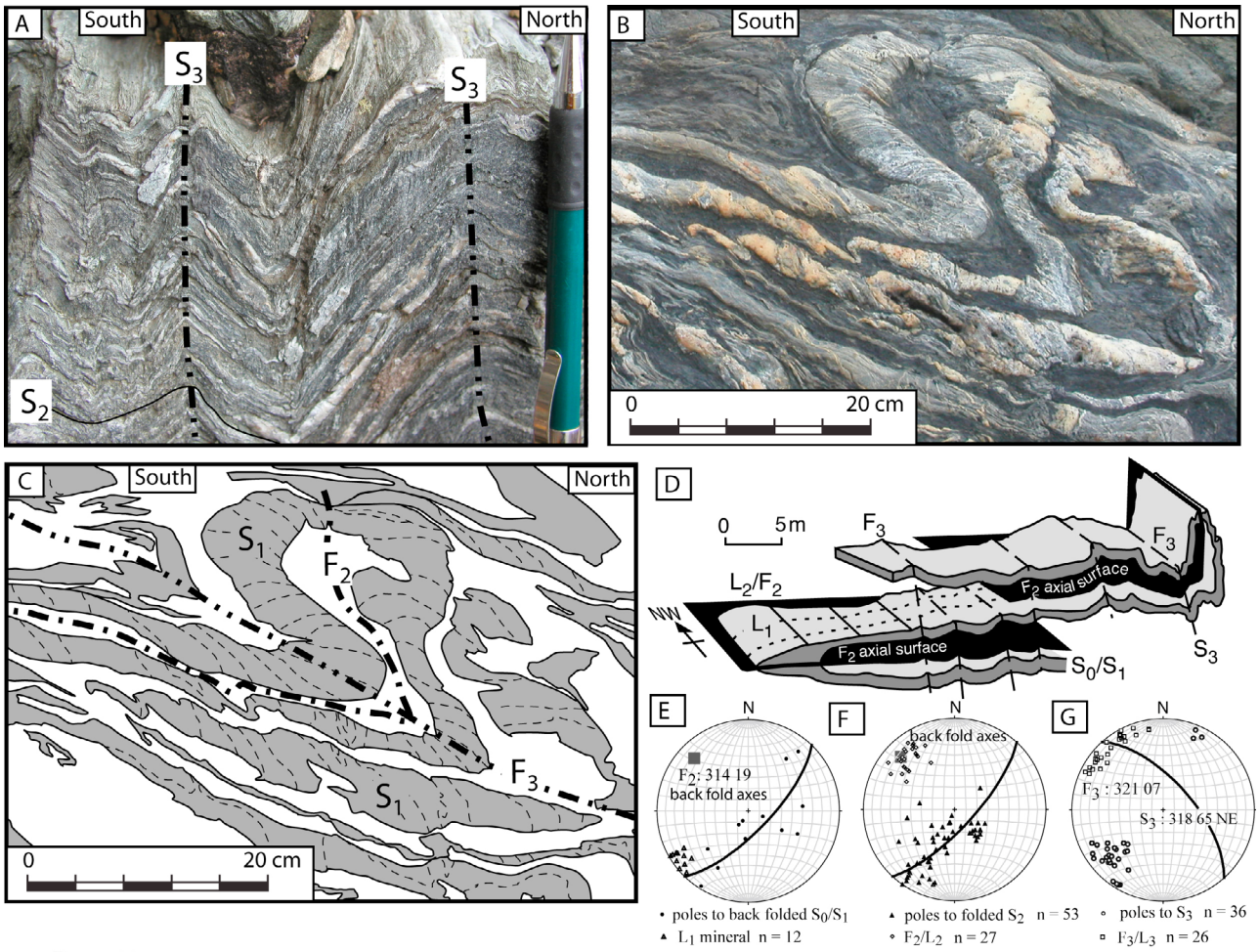

Figure 7. Cleavage-fold relationships in Seno Garibaldi. Photographs of S_3 and F_3 folds of S_2 (a) in areas of low strain where the folds are upright and chevron-shaped and (b) in areas of high strain near back thrusts where F_3 folds are tight and overturned to the south and SW. (c) Summary sketch of Figure 7b. (d) Block diagram summarizing the geometry of the two superposed folds in three dimensions. (e, f, and g) Lower hemisphere, equal-area stereoplots showing orientation data.

orthogneiss also were deformed and interfolded with the granitic orthogneiss. These mafic dikes are interpreted to have been emplaced during the opening of the Rocas Verdes basin [*Nelson et al.*, 1980]. Last, granitic rock of the Cretaceous Beagle suite intruded a section from the northern end of Bahía Pia to the Beagle Channel east of Caleta Olla (CO, Figure 2). These granite bodies lack penetrative foliations but are cut by late strike-slip and oblique-slip faults.

[24] Crosscutting relationships among the three igneous suites and groups of rock fabrics and folds allowed us to reconstruct a sequence of structures. The oldest structure is dismembered compositional layering (S_0) in basement schists, now deformed into tight intrafolial folds. In metapsammite layers, a poorly preserved spaced cleavage defined by aligned grains of flattened quartz and white mica parallels the axial planes of these folds (Figure 8a). This cleavage and the folds occur exclusively in the basement schists [see also *Nelson et al.*, 1980]. They are cut by the granitic dikes of the Darwin suite, indicating that they formed prior to the Late Jurassic opening of the Rocas Verdes basin. We therefore distinguish them from the younger structures that formed during basin closure and do not discuss them further.

[25] The dominant foliation is composite and includes at least two cleavages deformed by macroscopic overturned folds. Figure 8 summarizes the structural relationships between the fabrics and folds. The oldest of the two foliations (S_1) occurs mainly as curved inclusion trails of quartz, titanite and chlorite inside garnet porphyroblasts in the basement schists [*Kohn et al.*, 1993]. We observed this foliation in outcrop as discontinuous metapsammite layers in basement that are enveloped by an S_2 crenulation cleavage and are folded by tight F_2 folds that plunge ~60° to the west (Figure 10b). In quartz-rich layers, a penetrative quartz stretching lineation (L_1) occurs on folded S_1 planes. Sense of shear indicators, including oblique foliations and asymmetric recrystallized tails on quartz aggregates, indicate a top-to-the-northeast thrust sense on surfaces viewed parallel

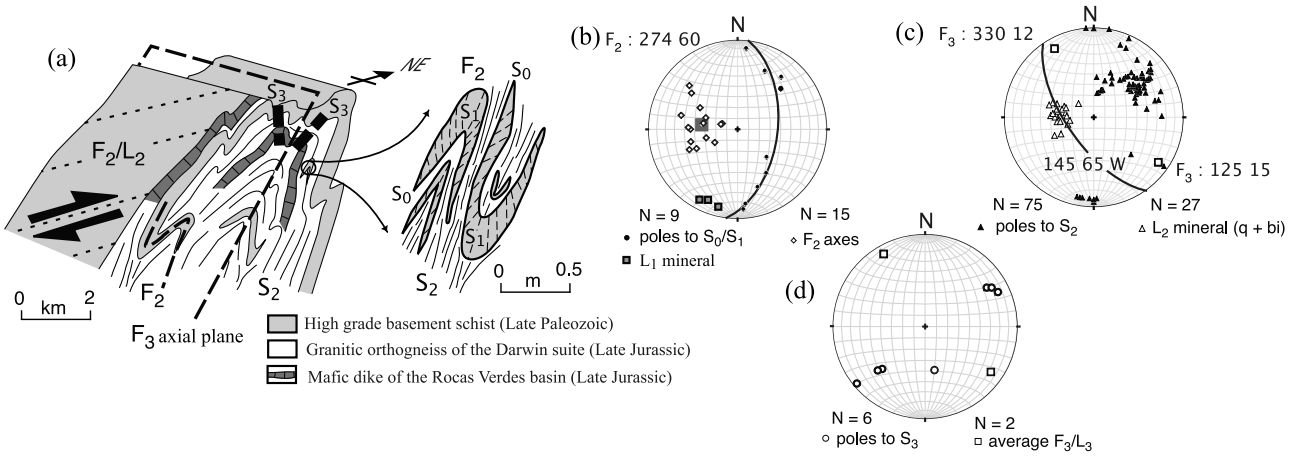

Figure 8. Fold-fabric relationships in the domain of high-grade metamorphic rocks in Bahía Pia. (a) Block diagram summarizing the geometry of superposed fabrics and folds in three dimensions. Inset shows the patchy preservation of S_1 in folded metapsammite layers in basement. (b, c, and d) Lower hemisphere, equal-area stereoplots showing orientation data.

to L_1 and perpendicular to S_1. Relationships preserved by this L_1-S_1 fabric reflect a cratonward thrust event that accompanied early prograde metamorphism. This interpretation is consistent with the conclusions of both *Nelson et al.* [1980] and *Kohn et al.* [1993], who indicated that prograde metamorphism accompanied the development of S_1. We discovered asymmetric structures that are consistent with continent-directed thrusting during this event.

[26] The second, and dominant, foliation (S_2) is a penetrative, closely spaced crenulation cleavage defined by aligned garnet, biotite, and muscovite, with or without clinozoisite, in metapelitic schists, and garnet, hornblende, clinozoisite, and plagioclase in amphibolite layers. S_2 in granitic orthogneiss of the Darwin suite is defined by aligned biotite, plagioclase, microcline, and quartz. Both staurolite and kyanite overgrow folded S_1 inclusion trails that are continuous with the S_2 crenulation cleavage in the matrix. This texture indicates that the peak conditions, represented by the growth of kyanite and staurolite, occurred synchronously with the formation of S_2, a conclusion also reached by *Nelson et al.* [1980] and *Kohn et al.* [1993].

[27] In most places, especially in metapsammite layers and granitic orthogneiss, a penetrative downdip and oblique quartz-biotite mineral lineation (L_2) occurs on S_2 cleavage planes (Figure 10c). This L_2 lineation is distinguishable from L_1 in that L_2 is not folded by F_2 folds. Where F_2 folds are present, L_2 is either parallel to or lies at a low angle to F_2 fold axes (Figures 10b and 10c). Boudinage and pinch and swell of dikes and quartz veins indicate that L_2 represents a true stretching lineation. Sense of shear indicators, including mica fish, C-S fabric, oblique quartz foliations and asymmetric recrystallized tails on plagioclase clasts, all indicate a top-to-the-northeast sense of shear on S_2 planes. This L_2-S_2 fabric defines a major mid to lower crustal shear zone that is at least a kilometer thick. The sense of shear indicators, combined with the textural evidence of synkinematic growth of kyanite and staurolite, indicates that prograde metamorphism occurred as basement and cover rocks were underthrust to the south and southwest beneath rocks that form part of the Rocas Verdes basin.

[28] The youngest foliation in the high-grade core is a widely spaced crenulation cleavage (S_3) associated with the retrogression of peak metamorphic assemblages [see also *Kohn et al.*, 1993]. This cleavage cuts S_2 and is defined by conjugate kink bands in mica-rich layers within the cores of two macroscopic folds (F_3) of the L_2-S_2 shear fabric (Figure 3e). These upright F_3 folds are overturned to the northeast and have shallowly plunging axes (Figure 10). The southernmost fold in Bahía Pia is a synform cored by pelitic basement; an antiform occurs at the northern end of the fjord. The northern limb of another synform between the northern end of Bahía Pia and Bahía Parry is cut by the Parry thrust (Figure 3e). This crosscutting relationship indicates that the Parry thrust postdated the thrusting that accompanied the development of S_1 and S_2.

[29] At the northern end of Bahía Pia, the L_2-S_2 fabric and the F_3 antiform are cut by granites of the Beagle suite; indicating that both folding and L_2-S_2 underthrusting occurred prior to or during pluton emplacement. The granite sheet trends southeast of Bahía Pia where it is exposed along the Beagle Channel east of Ventisquero Roncagli (R, Figure 2). Here it is cut by late strike-slip faults, indicating that the faulting is younger than F_3 folding. A narrow (several tens to a hundred meters thick) contact aureole characterized by sillimanite-bearing assemblages and, locally, migmatite in metapelitic schist, surround the pluton. The occurrence of these assemblages reflect an increase in metamorphic grade north of the Beagle Channel from greenschist facies near the mouth of Bahía Pia to sillimanite-bearing rocks at its northern end. A corresponding decrease in metamorphic grade occurs toward Bahía Parry. These metamorphic gradients are interpreted to be artifacts of late faults (normal in the south and thrust in the north) that form the boundaries of the high-grade core of southern Cordillera

Darwin. These late faults are associated with narrow (less than several hundred meters) zones where high-grade fabrics have been retrogressed to lower grade, greenschist facies fabrics.

3.5. Beagle Channel Fault Zone

[30] Each of the four domains contains arrays of strike-slip, oblique-slip, and normal faults that comprise the Beagle Channel fault zone. The highest strains are associated with strike-slip and transtensional faulting within one kilometer of the Beagle Channel. In this zone, all Cretaceous thrust-related folds and foliations are overprinted and recrystallized by ductile (greenschist facies) and brittle fabrics that record strike-slip, normal, and oblique-normal displacements. Top-down-to-the-south normal displacements are common on the northern side of the Beagle Channel, especially near Bahía Pia (Figure 2). Here, the normal faults consist of a protomylonitic foliation and a penetrative downdip quartz-mica mineral lineation on foliation planes. Sense of shear indicators, including chlorite fish, oblique foliations and asymmetric recrystallized tails (σ type) on feldspar grains, record a top-down-to-the-south normal sense of shear on surfaces oriented parallel to lineation and perpendicular to foliation [see also *Dalziel and Brown*, 1989]. Top-down-to-the-north normal displacements also are common along the northern shores of Isla Gordon, including in Bahía Romanche (BR, Figure 2). These faults define part of a large graben centered on the northern arm of the Beagle Channel [see *Menichetti et al.*, 2008, Figures 6 and 13]. Another large 4–5 km wide graben occurs in central Seno Ventisquero (Figures 2 and 3).

[31] Sinistral strike-slip and oblique-normal displacements are the dominant style of faulting in central Isla Gordon where faults are defined by narrow (tens of meters thick) zones of brittle and semibrittle fabrics composed of numerous minor fractures, veins and steep cleavages. Some faults parallel the contacts between gabbroic dikes and their host rock, although others offset these contacts by several tens of meters. The fault zone cleavages everywhere cut the older penetrative cleavage and folds that occur in the metasedimentary sequences, indicating that faulting postdates emplacement of gabbroic dikes.

[32] Another high-strain zone occurs at the southernmost end of Seno Ventisquero. Here, moderately dipping layers in gabbroic and metasedimentary rock are steepened to subvertical and tightly folded and faulted. This steep zone is an ~8 km thick greenschist facies shear zone (measured across strike) where steep ductile fabrics are cut by brittle strike-slip and oblique-slip faults (see descriptions of Punta Timbales by *Cunningham* [1995]). In contrast to the downdip orientation of mineral lineations in thrusts and normal faults, subhorizontal quartz stretching lineations occur on foliation planes near Punta Timbales. Asymmetric shear indicators, including C-S and C′ shear bands indicate a sinistral sense of shear.

[33] A third high-strain zone exhibiting left-lateral strike-slip displacements extends from Caleta Olla to northern Bahía Pia where strike-slip faults cut a metamorphic aureole of a Beagle suite pluton (Figure 2) [see also *Cunningham*, 1995]. Steep, upright folds occur within a few hundred meters of the Beagle Channel. These folds deform a retrogressed S_2 foliation that, several kilometers north of the coast, hosts relic kyanite and staurolite grains similar to those exposed at Bahía Pia. This zone of strike-slip faulting connects to the zone of normal faulting at the mouth of Bahía Pia where, along with the strike-slip system at Seno Ventisquero, it forms a ~10 km wide left step over centered on Bahía Pia.

4. Zircon Geochronology

4.1. Methodology

[34] The analysis of zircon in six samples (Figure 2) allowed us to determine the absolute ages of rocks representative of the Darwin and Beagle intrusive suites, and the maximum depositional age of the sedimentary fill of the Rocas Verdes terrane. All concentrates were prepared at the Departamento de Geología, Universidad de Chile, Santiago. U-Pb ages were obtained using SHRIMP I, II and RG at the Research School of Earth Sciences, Australian National University, Canberra. Measurement techniques followed those described by *Williams* [1998]. The probe standard was FC1. The data (Figures 9 and 10 and Data Set S1 in the auxiliary material) were processed using the SQUID Excel Macro of *Ludwig* [2001].[1] Uncertainties are reported at the 1σ level. Corrections for common Pb were made using the measured $^{238}U/^{206}Pb$ and $^{207}Pb/^{206}Pb$ ratios following *Tera and Wasserburg* [1972] as outlined by *Williams* [1998]. The $^{206}Pb/^{238}U$ ratios were used to obtain the ages reported here (Data Set S1). The geological time scale follows that of the IUGS-ICS (http://www.stratigraphy.org/cheu.pdf).

4.2. Results

[35] Sample 07K21 is from a micaceous quartzite collected from exposures of the Yahgan Formation at Bahía Tres Brazos (Figures 2 and 3a). The quartzite is folded and displays a steep spaced cleavage defined by aligned muscovite grains. Gabbroic dikes intruding the quartzite also display minor folds. Detrital zircon spectra from this sample were collected to determine a maximum depositional age for the sedimentary units of the Rocas Verdes basin terrane and to evaluate sources for the basin fill. The analysis of 61 grains (Figure 9a) yielded a detrital age distribution with a broad peak that can be unmixed into three groups of Late Jurassic age (Figure 9b). The dominant group yielded 152.60 ± 0.56 Ma (MSWD = 0.93) (auxiliary material Figure S1a). Two subordinate peaks also occur, with the youngest yielding an age of 147.7 ± 1.0 Ma (MSWD 0.52) (Figure 9c) and the oldest an age of 158.0 ± 1.2 Ma (MSWD 0.22) (Figure S1b). The younger result represents the maximum depositional age for the unit.

[36] Sample 07K25 is from a homogeneous, weakly foliated granitic dike that intrudes basement at the northern end of Seno Chair (Figure 2). The sample is from the contact aureole of a Beagle suite pluton and lies at the contact between Paleozoic metamorphic basement and Jurassic rift-related cover rocks of the Darwin suite. The sample was

[1] Auxiliary material data sets are available at ftp://ftp.agu.org/apend/tc/2009tc002610. Other auxiliary material files are in the HTML.

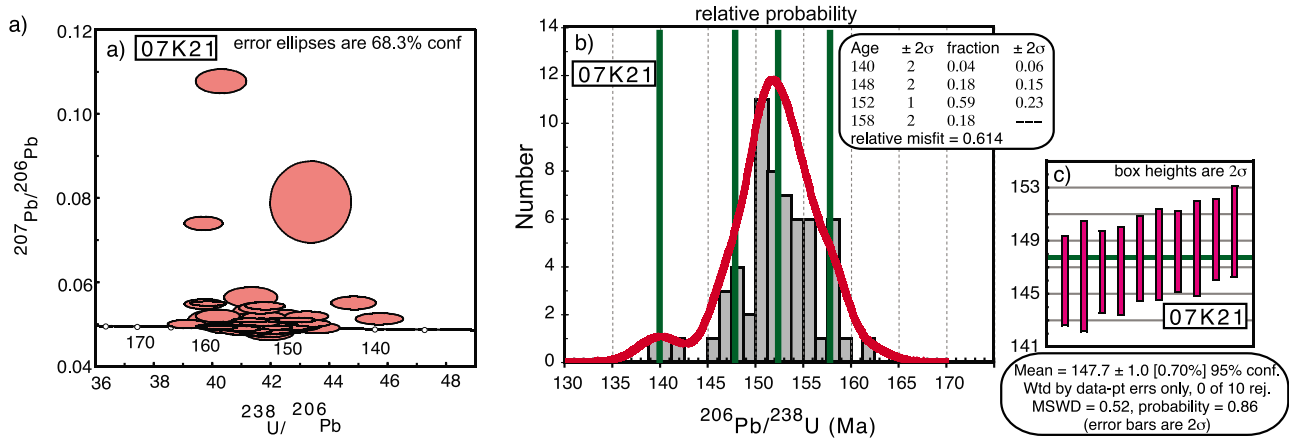

Figure 9. U-Pb isotopic data on zircon from sample 07K21 collected using SHRIMP I, II and RG at Australian National University. (a) Tera-Wasserberg concordia plot, (b) age versus probability diagram, and (c) calculated mean with errors reported at the 2σ level. Figures 2 and 3 show sample location.

collected to determine the age of rock into which the Beagle suite granitoids intruded and the age of the basement-cover contact at this locality. The analysis of 20 zircon grains (Figure 10a) yielded no sign of inheritance and provided an average igneous crystallization age of 154.2 ± 1.3 Ma (MSWD = 2.5). The elimination of three outliers provides an improved weighted average of 154.7 ± 1.0 Ma (MSWD = 1.3) (Figures 10b and 10c). These ages confirm that the granite belongs to the Darwin suite.

[37] Sample 07K51 is from a 0.5–1 m thick granitic dike that intrudes basement schist at the northern end of Seno Ventisquero (Figure 2). The dike cuts a penetrative schistosity in the basement that may predate structures formed during closure of the Rocas Verdes basin (see also section 3.4). Both the dike and the basement schistosity are folded by southwest vergent back folds. A second generation spaced cleavage defined by aligned biotite grains also is present in the dike and basement. We collected this sample to confirm that it belongs to the Late Jurassic Darwin suite and to facilitate a correlation of the basement-cover contact between fjords. The analysis of 20 zircon grains (Figure 10d) yielded a broad peak that can be unmixed into two groups (Figure 10e). The dominant peak yielded an average igneous crystallization age of 153.12 ± 0.93 Ma (MSWD = 0.82) (Figure 10f). A subordinate peak defined by four grains yielded an average crystallization age of 158.2 ± 1.8 Ma (MSWD = 0.37) (Figure S1c).

[38] Samples 07K60, 07K34, and 07K22A are from undeformed, locally megacrystic granitic plutons of the Beagle suite (Figures 2 and 3). Each of these plutons cuts thrust faults that formed during the obduction of Rocas Verdes oceanic sequences onto the South American continental margin. We collected these samples to determine the crystallization ages of the plutons and to place an upper age limit on obduction phase deformation. Samples 07K60 and 07K35 yielded the oldest ages. The analysis of 18 zircon grains from each sample produced late Cretaceous peaks. For sample 07K60 this peak produced a best fit igneous crystallization age of 85.89 ± 0.58 Ma (MSWD = 1.16) (Figures 10g, 10h, and 10i). For sample 07K34 it yielded a best fit age of 84.53 ± 0.48 Ma (MSWD = 0.64) (Figures 10j, 10k, and 10l). Sample 07K60 also produced one Jurassic and one Late Proterozoic age, and a subordinate peak yielded ages within the range 132–155 Ma (Figures 10h and S1d). Sample 07K22A yielded the youngest ages for the granites (Figures 10m, 10n, and 10o). The analysis of 15 grains generated a dominant peak (11 grains) and an average igneous crystallization age of 73.89 ± 0.50 Ma (MSWD = 0.69). Subordinate peaks include one ~89 Ma age, one Precambrian age and six Jurassic ages with a weighted mean of 155.3 ± 2.4 Ma (MSWD = 1.4) (Figures S1e and S1f). The subordinate peaks in these three samples most likely reflect inheritance.

5. Composite Structure and Shortening Estimates

5.1. Composite Structure

[39] Figure 11a shows a composite profile of Cordillera Darwin and south central Tierra del Fuego. To generate the southern part of this profile, we used the lateral continuity of structures along the Beagle Channel in combination with east-west changes in the depth of exposure to project features into the line of section. The northwesterly plunge

Figure 10. U-Pb isotopic data on zircon collected using SHRIMP I, II, and RG at Australian National University. (a, d, g, j, and m) Tera-Wasserberg concordia plots and (b, e, h, k, and n) age versus probability diagrams for samples 07K25, 07K51, 07K60, 07K34 and 07K22A, respectively. (c, f, i, l, and o) Calculated means with errors reported at the 2σ level. Blackened points in Figures 10j and 10k are excluded from age calculation. Figures 2 and 3 show sample locations.

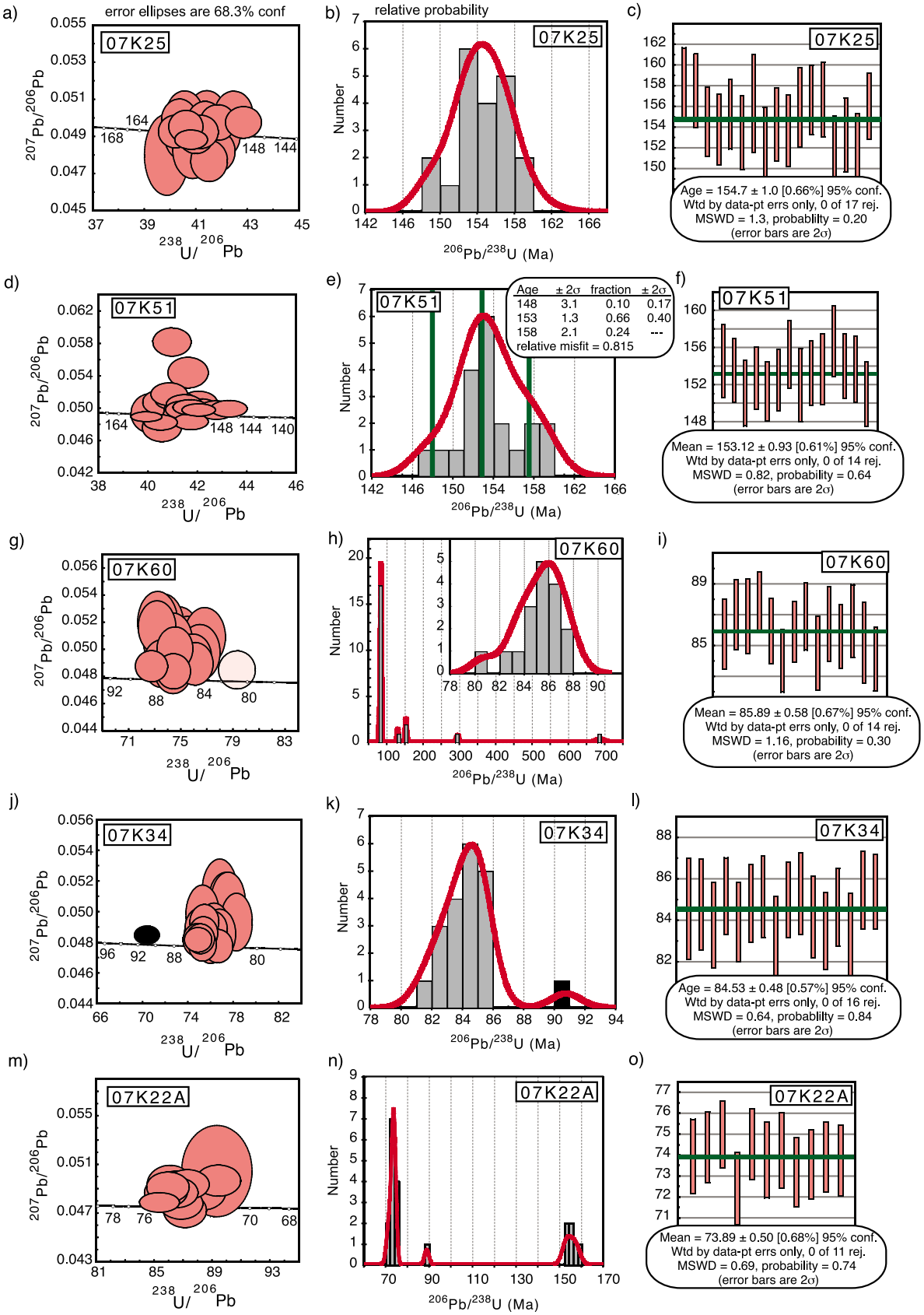
a)
error ellipses are 68.3% conf
07K25
$^{207}Pb/^{206}Pb$
$^{238}U/^{206}Pb$
b)
relative probability
07K25
Number
$^{206}Pb/^{238}U$ (Ma)
c)
07K25
Age = 154.7 ± 1.0 [0.66%] 95% conf.
Wtd by data-pt errs only, 0 of 17 rej.
MSWD = 1.3, probablilty = 0.20
(error bars are 2σ)
d)
07K51
e)
07K51
Age ± 2σ fraction ± 2σ
148 3.1 0.10 0.17
153 1.3 0.66 0.40
158 2.1 0.24 ---
relative misfit = 0.815
f)
07K51
Mean = 153.12 ± 0.93 [0.61%] 95% conf.
Wtd by data-pt errs only, 0 of 14 rej.
MSWD = 0.82, probability = 0.64
(error bars are 2σ)
g)
07K60
h)
07K60
i)
07K60
Mean = 85.89 ± 0.58 [0.67%] 95% conf.
Wtd by data-pt errs only, 0 of 14 rej.
MSWD = 1.16, probability = 0.30
(error bars are 2σ)
j)
07K34
k)
07K34
l)
07K34
Age = 84.53 ± 0.48 [0.57%] 95% conf.
Wtd by data-pt errs only, 0 of 16 rej.
MSWD = 0.64, probablilty = 0.84
(error bars are 2σ)
m)
07K22A
n)
07K22A
o)
07K22A
Mean = 73.89 ± 0.50 [0.68%] 95% conf.
Wtd by data-pt errs only, 0 of 11 rej.
MSWD = 0.69, probability = 0.74
(error bars are 2σ)

Figure 10

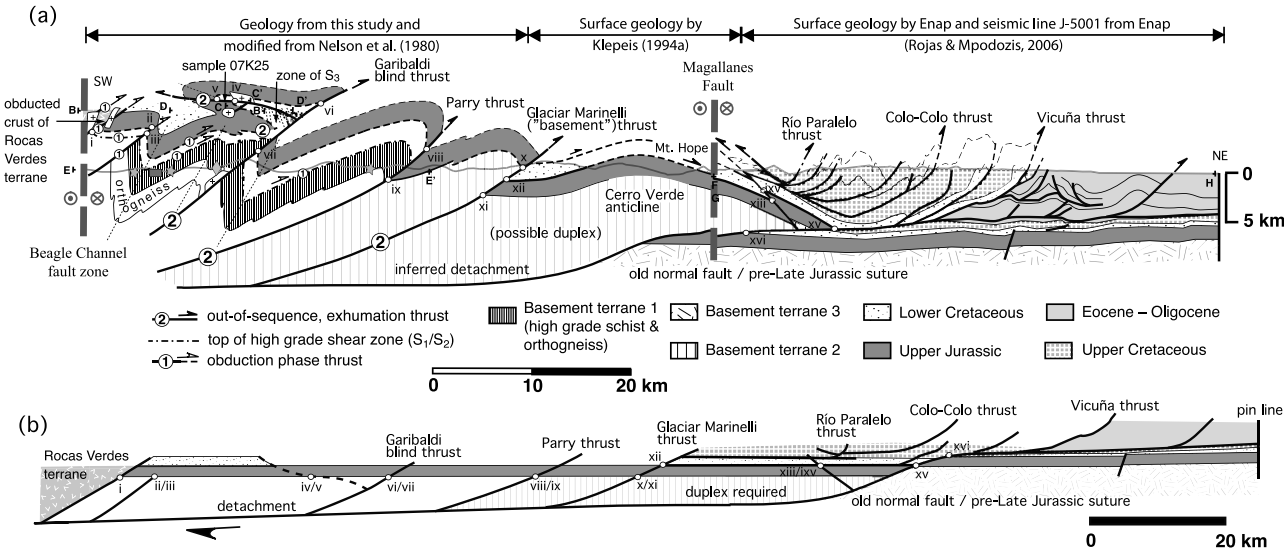

Figure 11. (a) Composite profile of Cordillera Darwin and south central Tierra del Fuego. Southern part of profile shows the location of sections B-B′, C-C′, D-D′, and E-E′ in Figure 3. The northern part is from ENAP industry profile J-5001 interpreted by *Rojas and Mpodozis* [2006]. Paleozoic suture is from *Hervé et al.* [2010]. Figure 13 shows location of profiles E-F and G-H. Faults and folds labeled 1 and 2 represent obduction and exhumation phases, respectively. White dots with lower case Roman numerals indicate points used to restore the section. Stars, rectangle, and diamonds along profile E-E′ represent occurrences of staurolite, kyanite, and sillimanite mineral assemblages (see also Figure 6b). (b) Restored section. North of the Magallanes fault is from *Rojas and Mpodozis* [2006]. Duplexes in Upper Cretaceous rocks and below Cerro Verde anticline are omitted.

(15°–20°, Figure 5c) of F_2 back folds in senos Ventisquero and Chair result in an increase in the depth of exposure from west to east. The structures in profile B-B′ project a few hundred meters below, and several kilometers south of, the back thrusts shown in profile C-C′ (Figure 3b). The depth of exposure shown in profile C-C′ also projects a few hundred meters beneath that shown in D-D′. This latter relationship is evident because the footwall of the back thrust in profile C-C′ is composed mostly of basement rock, whereas in Seno Garibaldi (profile D-D′) it is composed of cover rocks. This indicates that Seno Garibaldi exposes an antiformal culmination in the domain of back thrusts.

[40] Above the back thrust in profile C-C′ we used the ages obtained from sample 07K25 (154.7 ± 1.0 Ma) to locate the basement-Tobifera contact (Figures 2, 3c, and 3d). This location agrees with that inferred by *Nelson et al.* [1980]. We also used the crystallization age obtained from sample 07K51 (158.2 ± 1.8 Ma) to estimate the location of this same contact below the back thrusts in Seno Ventisquero (Figures 2 and 3b). An age from near the basement-Tobifera contact above the back thrust at Seno Garibaldi (159.4 ± 1.4 Ma, sample GA17B, Figure 2) is reported by *Hervé et al.* [2010]. These correlations indicate that the amount of displacements on the back thrusts is relatively small (<5 km).

[41] A large increase in the depth of exposure occurs east of Seno Garibaldi. This increase results partly from displacements on a late normal fault of the Beagle Channel fault zone that uplifted the high-grade rocks of Bahía Pia in its footwall (Figures 2 and 3e). Rocks in the hanging wall show that obduction phase thrusts in the Tobifera Formation once lay on top of the high-grade schists. In addition, back folds in Seno Cerrado plunge moderately to the northwest below the exposures in Seno Garibaldi. These relationships indicate that the high-grade rocks project beneath the cover rocks exposed to the west. Over a distance of ~20 km, the ~20° plunge of folds suggests that profile E-E′ projects 6–7 km below the base of the back thrusts on profile D-D′. This agrees with profile E-E′ of *Nelson et al.* [1980]. East of Bahía Pia, the high-grade exposures project beneath structures exposed east of Ventisquero Roncagli (R, Figure 2), which results from a change in the plunge of folds from northwest to southeast [*Cunningham*, 1995] and creates an elongate dome of high-grade rocks (Figure 6b).

[42] The exposure of high-grade rocks in bahías Pia and Parry (profile E-E′) helped us to correlate structures between southern and northern Cordillera Darwin. This continuous wedge of high-grade rock lies structurally below the back thrusts in Seno Garibaldi and structurally above the Parry thrust (Figures 3e and 11a). The transition below the back thrusts into the high-grade rocks is partly exposed in senos Chair (Figure 3c) and Cerrado [*Nelson et al.*, 1980]. Profile C-C′ shows that the back thrusts truncate northeast vergent (obduction phase) thrusts. Below this depth, several other inferences can be made. First, exposures at the southern end of Bahía Pia (Figures 2 and 3e) indicates that low-grade rocks of the Tobifera Formation were placed on top of the high-grade rocks by a northeast vergent thrust. Second, the presence of the NW trending band of S_3 crenulation cleavage and F_3 folds west of Seno Garibaldi (Figure 6a) suggests the presence of a blind northeast vergent thrust that separates the

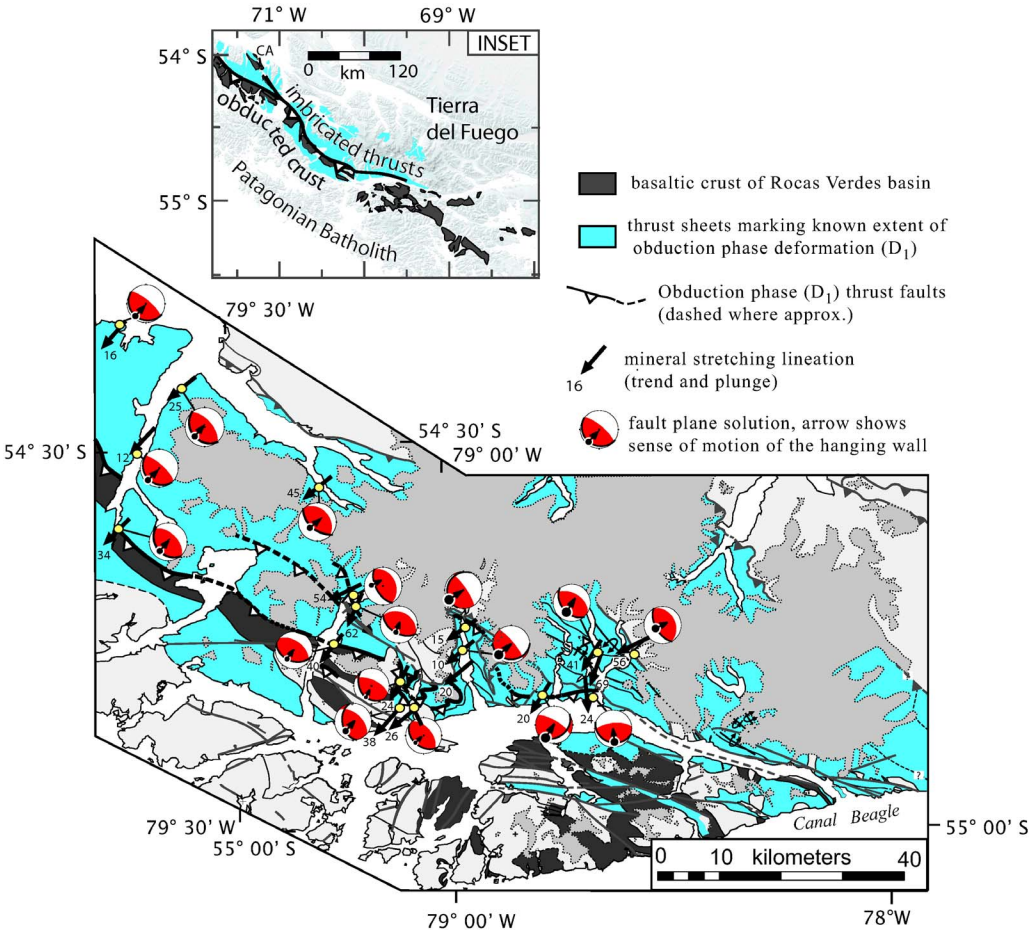

Figure 12. Tectonic map showing the regional extent and kinematics of obduction thrusts (dark black lines with white triangles). Fault plane solutions for thrusts are shown on lower hemisphere equal-area stereoplots that incorporate data on fault plane orientation (bold great circles), mineral striae (black dots), and sense of motion of the hanging wall (arrow). Data define a narrow (~ 60 km wide) orogenic wedge that formed prior to ~86 Ma (inset). CA, Isla Capitán Aracena.

back thrusts from the high-grade rocks (Figures 6a and 11a). In section 3.3 we show that the kinematic evolution of the S_3 cleavage is linked to back thrusting. In support of this interpretation, the northern boundary of the zone of S_3 crenulation cleavage is exposed between Bahía Brookes and Seno Agostini (Figure 6a) where it is a northeast vergent thrust fault that places basement over cover rocks. A similar emergent thrust is the Parry thrust, which also uplifts basement (Figure 2). These thrusts form a bivergent wedge that is one of the defining structural characteristics of Cordillera Darwin.

[43] Below the Parry thrust there is a change in the nature of Paleozoic basement (Figure 11a). *Hervé et al.* [2010] used detrital zircon ages to postulate the presence of an old pre-Late Jurassic suture that separates distinctive basement terranes. The suture may lie approximately beneath the Magallanes fault zone. These authors also showed that the protoliths of the high-grade schists in Cordillera Darwin comprise a number of small late Paleozoic blocks with independent magmatic sources. Rocks from the hanging wall of the Parry thrust display Cambrian and Devonian peaks in the range 575–330 Ma and 590–480 Ma (Figure 3e). In the footwall, the age spectra indicate a mainly pre-Devonian provenance with major peaks at ~400 Ma and 470–450 Ma. We illustrate these distinctive basement terranes and suggest that the Parry thrust may reactivate either another pre-Jurassic suture or a Jurassic normal fault.

[44] North of the Parry thrust, we combined our data with structures mapped by previous authors. We traced the Cerro Verde anticline and Glaciar Marinelli (basement) thrust (Figure 11a), to the northern end of Bahía Parry. This includes the location of the Tobifera-basement contact in the hanging wall of the Parry thrust, which is exposed east of the fjord (Figure 2). Geologists from the Chilean National Petroleum Company (Sipetrol-ENAP) traced similar structures to the west into Bahía Brookes [*Rojas and Mpodozis*, 2006]. The structure of Bahía Brookes (Figures 6a and 13) is modified from *SERNAGEOMIN* [2002] using original mapping by L. Rojas and kinematic data by K. Klepeis.

[45] East and north of Seno Almirantazgo (Figure 2), the profile in Figure 12 includes information from ENAP seismic reflection profile J-5001 and surface geology collected

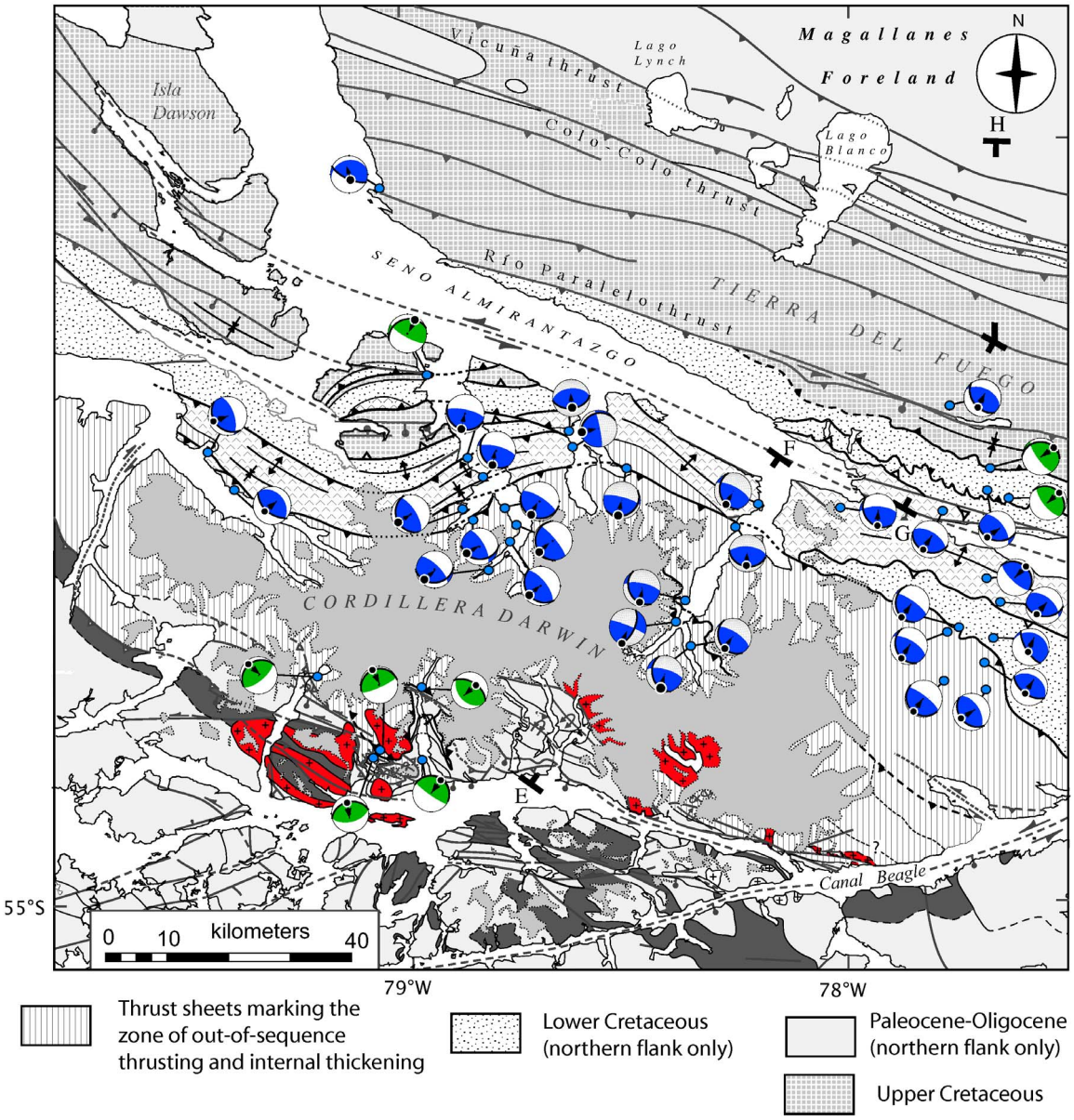

Figure 13. Tectonic map showing the regional extent and kinematics of out-of-sequence phase thrusts in Cordillera Darwin. Beagle suite granite is shown in red. Fault plane solutions for thrusts are shown on lower hemisphere equal-area stereoplots that incorporate data on fault plane orientation (bold great circles), mineral striae (black dots), and sense of motion of the hanging wall (arrow). Fault slip data define a bivergent wedge bounded on the south by back thrusts (green solutions) and on the north by basement-cored northeast vergent thrusts. Figure 11 shows profiles E-F and G-H. Geology of the Magallanes foreland fold-thrust belt in central Tierra del Fuego is modified from *SERNAGEOMIN* [2002].

by ENAP geologists [*Rojas and Mpodozis*, 2006]. Information obtained from wells drilled by this company constrain the depth to metamorphic basement. The main features represented include three major forward breaking thrusts; the Río Paralelo, the Colo-Colo, and the Vicuña faults (Figures 11a and 13); which comprise a thin-skinned foreland fold-thrust belt that formed between Paleocene and Eocene times [*Alvarez-Marrón et al.*, 1993; *Rojas and Mpodozis*, 2006]. A ramp and detachment are inferred below the Cerro Verde anticline to balance the section [see also *Klepeis*, 1994a; *Kley et al.*, 1999; *Rojas and Mpodozis*, 2006].

5.2. Minimum Shortening Estimates

[46] Previous estimates of shortening in the Magallanes fold-thrust belt are sparse. *Alvarez-Marrón et al.* [1993] used ENAP seismic lines to estimate ~30 km (60%) of shortening

north of the Colo-Colo thrust in central Tierra del Fuego. *Kley et al.* [1999] combined data reported by *Alvarez-Marrón et al.* [1993] and *Klepeis* [1994a] to suggest ~83 km (~52% shortening) north of the Glaciar Marinelli thrust. One of the few attempts to estimate shortening across the entire orogen was reported by *Kraemer* [2003], who suggested a minimum of 300 km and a maximum of 600 km. This latter estimate was hindered by a paucity of data from the hinterland.

[47] The uplifted rocks of the Upper Jurassic Tobifera Formation, and their relative continuity across thrusts (Figure 11b), provides a means to obtain the first, albeit crude, estimate of the minimum amount of shortening recorded by thrusts and back thrusts in Cordillera Darwin. To obtain an estimate, we used a simple linear (bed length) restoration to reconstruct the profile shown in Figure 11a following established methods [*Dahlstrom*, 1969; *Elliott*, 1983; *Marshak and Mitra*, 1988]. The assumptions included (1) Lower Cretaceous units thicken to the southwest, including across a reactivated normal fault below the Magallanes fault trace (section 5.1), (2) a detachment exists beneath Cordillera Darwin, and (3) an overall forward propagating system best explains the sequence of events. Area or volume balancing is beyond the scope of this paper and is not warranted by the quality of the data. We used the base of the Tobifera Formation as a marker horizon because it is exposed across thrusts on both sides of Cordillera Darwin. A regional pin line lies near Lago Blanco (Figure 13), and corresponds to that used by others. Loose lines for each thrust sheet are oriented perpendicular to bedding.

[48] The results of our analysis suggest that a minimum of ~50 km of horizontal shortening (~70%) in cover rocks is accommodated between the Beagle Channel and Seno Almirantazgo (Figure 13). This estimate excludes all shortening recorded by older obduction phase structures, including underthrust continental crust, because of a lack of markers. A duplex in basement below the Cerro Verde anticline is required to balance the shortening in cover rocks (Figure 11b). North of Seno Almirantazgo, *Rojas and Mpodozis* [2006] and *Kley et al.* [1999] reported at least ~50 km of additional thin-skinned shortening above the Tobifera Formation, bringing the minimum amount of shortening in the Magallanes fold-thrust belt to at least 100 km.

6. Synthesis and Discussion

6.1. Opening the Rocas Verdes Basin

[49] The detrital zircon spectra from sample 07K21 (Figure 2) provide a maximum depositional age of ~148 Ma for the synrift sedimentary sequences (Yahgan Formation) on Isla Gordon (Figure 9). This age is compatible with published magmatic and detrital zircon ages from the northern part of the Rocas Verdes basin, indicating rifting between 152 and 142 Ma [*Calderón et al.*, 2007]. This interval comes from ~150 Ma ages on dacitic and plagiogranite dikes that cut pillow basalt successions at Cordillera Sarmiento, west of Puerto Natales (S, Figure 1) and ~148 and ~142 Ma detrital zircon ages from silicic pyroclastic rocks interpreted to have been deposited simultaneously with rifting. The near identical age we obtained from the synrift sequences into which mafic units of the Rocas Verdes sequences intruded hundreds of kilometers south of Cordillera Sarmiento precludes interpretations that the Rocas Verdes basin opened by unzipping from south to north [*Stern and de Wit*, 2003]. Instead, the similar ages suggest that the basin opened approximately simultaneously along its length in latest Jurassic time.

[50] The older detrital zircon peaks at ~158 and ~153 Ma in sample 07K21 (Figure 9b and auxiliary material Figures S1a and S1b) suggest that Upper Jurassic igneous rocks were a significant source of detritus into the Rocas Verdes basin. These ages correspond to those obtained from the Darwin granite suite (samples 07K51 and 07K25 in this study) and a period of 157–153 Ma rift-related silicic volcanism represented by the Tobifera Formation (V3 phase of *Pankhurst et al.* [2000]). Muscovite- and garnet-bearing leucogranites of roughly the same age (157–145 Ma) also occur along the eastern edge of the Patagonian Batholith north of the Magellan Straits [*Hervé et al.*, 2007]. No evidence exists for an active magmatic arc south of the straits at this time [*Mpodozis and Rojas*, 2006] (Figure 14a).

6.2. Continental Underthrusting and Obduction of Quasi-Oceanic Crust

[51] Crosscutting relationships between five Beagle suite plutons and thrust faults define two distinctive stages of Rocas Verdes basin closure. The granites cut all fabrics and folds associated with the obduction of the Rocas Verdes basaltic floor, thus establishing obduction as one of the first events to occur as the basin collapsed [*Nelson et al.*, 1980]. Below, we argue that the structures and metamorphic mineral assemblages preserved in an exhumed middle to lower crustal shear zone in Cordillera Darwin suggest that this obduction was accompanied by south directed subduction of the oceanic Rocas Verdes basin floor, followed by the underthrusting of South American continental crust to depths of ~35 km beneath a coeval volcanic arc.

[52] The range of ages we obtained from samples 07K22A, 07K60, and 07K34 indicates that obduction must have occurred prior to ~86 Ma. This result reflects a refinement of previously reported ages from Beagle Suite plutons, which typically yielded large errors (see *Hervé et al.* [1984] and compilation by *Kohn et al.* [1995]). It also is compatible with stratigraphic evidence and detrital zircon data from the northern part of the Magallanes foreland basin, which suggest that foreland sedimentation is no older than 92 ± 1 Ma [*Fildani et al.*, 2003], although thrusting most likely initiated earlier [see also *Kohn et al.*, 1995; *Calderón et al.*, 2007].

[53] Our work defines the regional extent of obduction phase structures and establishes the kinematic relationships among thrusts in adjacent fjords. Figure 12 shows fault plane solutions that illustrate the displacements involved in the obduction of basaltic (quasi-oceanic) crust (dark gray) on top of Lower Cretaceous rock and Paleozoic continental basement (blue). The solutions are a convenient way of preserving the three dimensionality of the displacements and displaying their spatial distribution. Each solution incorporates the orientation of the fault plane, the sense of shear, and the orientation of quartz-mica mineral lineations and

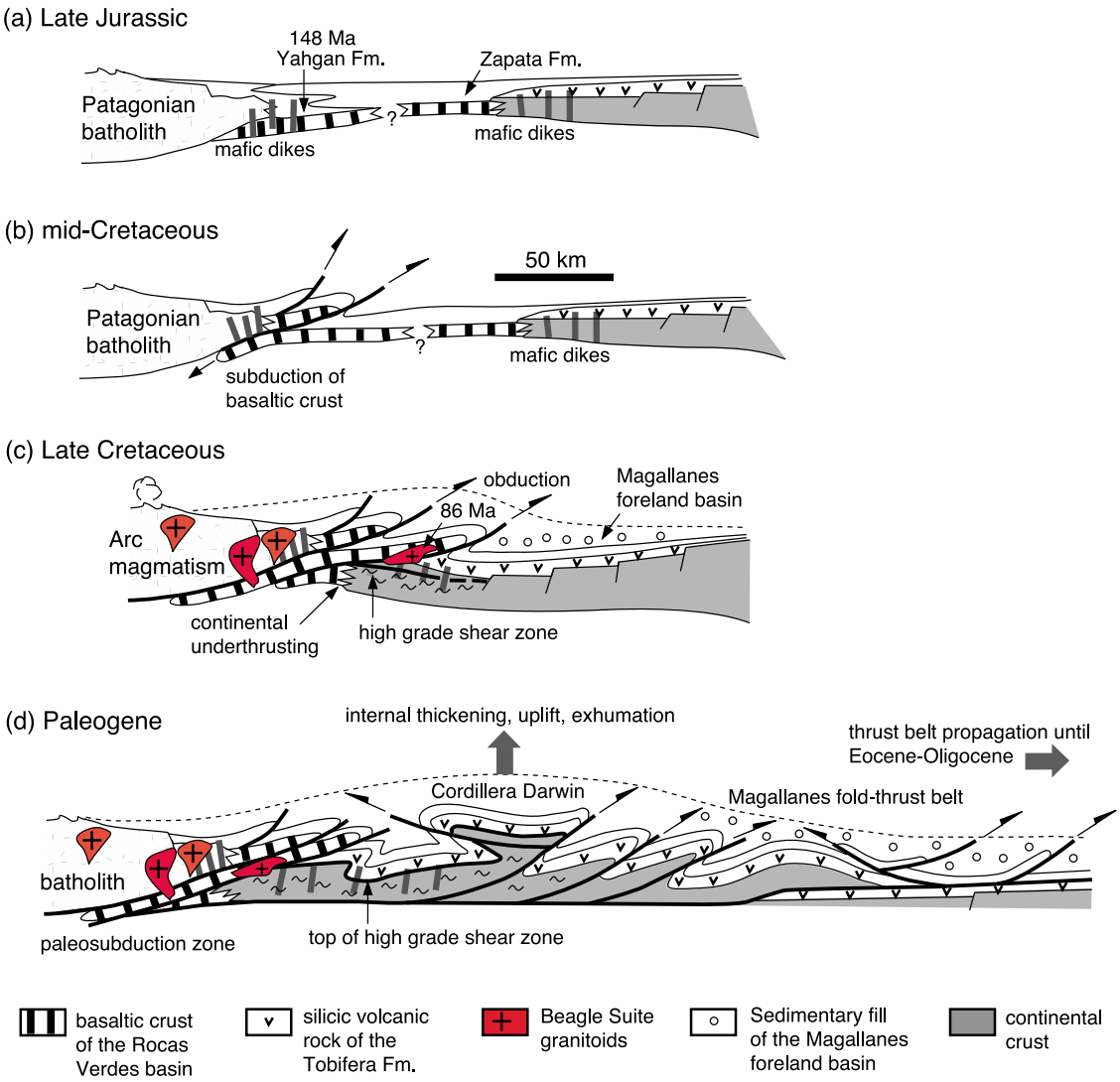

Figure 14. Cartoon summarizing the Late Jurassic-Paleogene evolution of the Rocas Verdes basin, Cordillera Darwin, and the Magallanes foreland fold-thrust belt at the latitude of Tierra del Fuego. (a) Rifting, diking, and bimodal volcanism forms the quasi-oceanic Rocas Verdes rift basin by the Late Jurassic. The basin fill thickens to the south, its width is uncertain, and arc magmatism is absent. (b) Compression initiates by ~100 Ma, leads to subduction of the basaltic floor beneath the batholith, and forms a narrow thrust wedge composed mostly of mafic floor fragments and deformed volcanic and sedimentary basin fill. (c) As closure continues, thinned continental crust and sequences of silicic volcanic rock (i.e., the Tobifera Formation) are underthrust beneath the thrust wedge, forming the high-grade shear zone exposed at bahías Pia and Parry and resulting in the uplift and obduction of the mafic floor of the basin prior to ~86 Ma. Arc magmatism, crustal melting, and emplacement of Beagle suite granitoids result from the underthrusting. Crustal loading and flexure create the Magallanes foreland basin (Figure 12 shows map view). (d) Collision between the Patagonian batholith and South American continental crust results in internal thickening, uplift, and exhumation of hinterland thrusts in Cordillera Darwin. In response to this thickening of the internal part of the wedge, the Magallanes fold-thrust belt propagates into the foreland, terminating by the Eocene-Oligocene (Figure 13 shows map view). Late Tertiary strike-slip faults have been omitted from the profiles for simplicity.

striae (methods described by *Marrett and Allmendinger* [1990]). The data show that the initial stage of Rocas Verdes basin closure formed a narrow (~60 km) thrust wedge (Figure 12, inset) that accommodated a nearly uniform continent-vergent sense of motion. The involvement of the Upper Jurassic Tobifera Formation in these thrusts (profiles C-C′, D-D′, and E-E′) indicates that the wedge must have been detached below the base of this unit.

However, the absence of Upper Jurassic zircons in the early detrital record of the Magallanes foreland basin [*Romans et al.*, 2010] indicates that thrust sheets uplifting the Tobifera Formation were not emergent and eroding during this initial stage. This suggests that the entire system lay below sea level and the Magallanes foreland basin was receiving sediment derived mostly from rock units at shallower depths, such as from the Yahgan and Zapata formations. The interpretation also is consistent with analyses of the provenance of the Upper Cretaceous Punta Barrosa Formation, further north, in the Última Esperanza region, where peaks in detrital zircon age distribution indicate that the exhumation and incorporation of Upper Jurassic igneous rocks into the foreland basin was established by ~80 Ma [*Romans et al.*, 2010]. Nevertheless, these correlations and comparisons are tentative because of the large distance between the study area in this paper and Última Esperanza region.

[54] The results presented here provide a means to correlate structures east and west of Seno Garibaldi. Crosscutting relationships between a Beagle suite pluton and the composite S_1/S_2 fabric that defines the middle to lower crustal shear zone at Bahía Pia indicate that this structure also formed prior to emplacement of the granites (section 3.4). Fault plane solutions indicate kinematic compatibility between movement on the midcrustal thrust and on the shallow upper crustal thrusts exposed farther west. Continental underthrusting at this time is recorded by the presence of thrust fabrics in Bahía Pia that were coeval with moderate high pressure upper amphibolite facies metamorphism. We interpret the midcrustal thrust as the deepest of several faults that formed during this early phase as a consequence of the south directed subduction of the Rocas Verdes basin floor and underthrusting of South American continental crust to depths of ~35 km beneath a coeval volcanic arc. In the study area, this arc is represented by the plutons of the Beagle suite [see also *Mpodozis and Rojas*, 2006]. Virtually no oblique-slip or strike-slip motion is evident on any thrust surfaces, which is consistent with the crosscutting relationship between the thrusts and younger strike-slip and oblique-slip faults. These results also are compatible with previous interpretations of the Cretaceous subduction of the mafic floor of the Rocas Verdes basin to the south beneath the Patagonian batholith [*Cunningham*, 1995; *Kraemer*, 2003; *Mpodozis and Rojas*, 2006].

[55] These relationships provide a possible explanation of the cause of obduction during closure of the Rocas Verdes basin. Deformed fossils indicate that shortening in the southernmost Andes had initiated by ~100 Ma (Figure 14b) [*Halpern and Rex*, 1972; *Dott et al.*, 1977]. The cause of the shift from rifting to compression is unknown, but commonly is attributed to changes in absolute plate motions and subduction dynamics as the South Atlantic Ocean opened during the Early Cretaceous [*Dalziel*, 1986; *Jokat et al.*, 2003; *Calderón et al.*, 2007]. After compression commenced, the thin crust and basaltic composition of the Rocas Verdes basin promoted the subduction of its floor southward beneath the Patagonian batholith (Figure 14b). This process formed a narrow thrust wedge initially composed of deformed volcanic and sedimentary basin fill and swarms of steep Jurassic mafic dikes. The presence of these dikes on both sides of the basin (Figure 14a) suggest that diking formed an important part of the process of welding basaltic crust to continental crust during rifting. As closure progressed, and the basaltic crust was consumed, sequences of Upper Jurassic silicic volcanic rock and thinned continental crust approached the subduction zone and were underthrust beneath the nascent thrust wedge (Figure 14c). This change in the composition of underthrust material, from quasi-oceanic basaltic crust to the thicker and more buoyant continental material, resulted in increased shortening, uplift, and obduction of basaltic crust prior to ~86 Ma (Figure 14c). The high-grade ductile shear zone exposed in bahías Pia and Parry helped facilitate underthrusting during this time. We also suggest that underthrusting helped fuel arc magmatism and crustal melting, leading to the emplacement of Beagle suite granitoids. Expansion of the thrust wedge also increased crustal loading and created the flexural Magallanes foreland basin. This sequence illustrates how variations in the composition and structure of the Rocas Verdes basin promoted continental underthrusting and obduction in a back arc setting.

6.3. Internal Thickening and Growth of a Bivergent Wedge

[56] Following obduction, another period of major thrust faulting thickened and imbricated basement and cover rocks in Cordillera Darwin. This event formed a bivergent wedge cored by high-grade rocks [see also *Mpodozis and Rojas*, 2006]. The southern boundary of the wedge coincides with the back thrusts mapped in senos Chair and Garibaldi (Figures 3c and 3d). The northern side is marked by three northeast vergent thrusts that include the emergent Parry and Glaciar Marinelli thrusts and the blind Garibaldi thrust (Figure 11a). All of these structures cut obduction phase thrusts, including the ductile shear zone exposed in bahías Pia and Parry, and formed out of sequence with respect to several décollements in northern Cordillera Darwin (white triangles on Figure 13) [see also *Klepeis*, 1994a]. All are associated with retrogression of the high-grade mineral assemblages and their uplift relative to basement in the foreland (Figure 11a). These relationships suggest that displacement on these thrusts, combined with erosion, resulted in the rapid exhumation of basement and Upper Jurassic igneous rocks in Cordillera Darwin [*Barbeau et al.*, 2009; *Gombosi et al.*, 2009]. This interpretation is consistent with provenance analyses of the Tres Pasos and Dorotea formations in the northern part of the Magallanes foreland basin, which indicate that the uplift and denudation of Upper Jurassic igneous rocks was occurring by ~80 Ma and that these rocks were a significant source of detritus by ~70 Ma [*Romans et al.*, 2010].

[57] Back thrusts similar to those mapped in the south also form pop ups above large northeast vergent thrusts on the northern side of Cordillera Darwin. Two of these occur in Bahía Brookes where they imbricate Upper Cretaceous-Tertiary sedimentary rock (Figure 13) [*Rojas and Mpodozis*, 2006]. Two others occur north of Lago Fagnano [*Klepeis*, 1994a] where they display tight, south vergent folds and

moderately north dipping crenulation cleavages like those at Seno Garibaldi. These relationships show that the formation of minor back thrusts above larger forward breaking thrusts was an important process during this postobduction phase of out-of-sequence thrusting and exhumation.

[58] The exact age of each out-of-sequence thrust and back thrust is uncertain. However, several relationships suggest that they all postdate emplacement of the Beagle suite granites and some record Paleocene-Eocene motion. Movement on the Glaciar Marinelli thrust has been inferred to be Eocene on the basis of U-Pb detrital zircon spectra and provenance data reported by *Barbeau et al.* [2009] and thermochronology reported by *Gombosi et al.* [2009]. This interpretation is consistent with relationships from Bahía Parry where late Cretaceous Beagle granites intruding basement have been displaced along the Parry thrust. The presence of faulted pebble conglomerates and coarse-grained turbidites of Paleocene or younger age unconformably overlying the Upper Cretaceous Punta Barrosa Formation at the northern end of Bahía Brookes suggests that back thrusting there also occurred after the Paleocene. Farther south in Cordillera Darwin, $^{40}Ar/^{39}Ar$ cooling ages reported by *Kohn et al.* [1995] indicate a period of cooling (250°C–200°C) and exhumation from ~61 to ~40 Ma that coincides with this period as the thrust belt propagated into the Magallanes foreland.

[59] In southern Cordillera Darwin, structural relationships suggest that back thrusting also occurred during Paleogene times. At the north end of Seno Chair (Figure 2), a back thrust cuts the contact aureole of a Beagle suite pluton (Figure 3c). The pluton itself lacks a penetrative subsolidus foliation, suggesting that the back thrusts preferentially were partitioned into the weaker fine-grained schist rather than in the coarse-grained granite. In support of this view, thin sections of muscovite schist within the contact aureole of the granite show a well-developed shear fabric and no evidence of the annealing of quartz expected if the pluton intruded after back thrusting. Available argon thermochronology on muscovite from the region [*Kohn et al.*, 1995] indicates that the oldest cooling ages are approximately 70 Ma. We suggest that this represents a lower limit on the age of back thrusting. This interpretation differs from that of *Nelson et al.* [1980], who interpreted back thrusting to have accompanied prograde metamorphism and tectonic burial to midcrustal depths. Our interpretation is consistent with structural data indicating the back thrust is not a major structure but one that records small (<5 km) displacements above a larger forward breaking thrust.

[60] These relationships indicate that many of the large thrusts in Cordillera Darwin, including the back thrusts, formed during a period of renewed Paleogene shortening following obduction. Figure 14d illustrates a possible explanation for this renewed shortening, which marks the final stage of Rocas Verdes basin collapse. The final stage was characterized by a back-arc collision between the Patagonian batholith and the thick crust of the adjacent South American continent as the two sides of the Rocas Verdes basin finally met. This collision slowed underthrusting beneath the batholith and resulted in out-of-sequence thrusting, internal thickening, uplift, and exhumation in Cordillera Darwin. Following these events, the Magallanes fold-thrust belt propagated rapidly into the foreland, suggesting that this sudden growth occurred to maintain the taper of a wedge that changed shape as a result of the internal thickening. Similar Coulomb wedge processes [*Davis et al.*, 1983; *Dahlen*, 1990] that can drive lateral growth in thrust belts and accretionary wedges also have been suggested for a part of the Magallanes fold-thrust belt in Argentina [*Torres Carbonell et al.*, 2010].

6.4. Strike-Slip and Oblique-Slip Faulting

[61] Everywhere we observed them, strike-slip, normal, and oblique-slip faults cut all thrust faults and folds indicating that they are the youngest style of faulting in the Beagle Channel region. Crosscutting relationship between these faults and granite plutons of the Beagle suite, and the subsolidus texture of all fault-related fabrics, indicate that strike-slip faulting occurred following granite intrusion. The age of the youngest Beagle suite pluton (sample 07K22A) indicates that the faulting must be less than ~73 Ma. U-Pb detrital zircon geochronology and thermochronologic data published by *Barbeau et al.* [2009] and *Gombosi et al.* [2009], respectively, suggest that the faulting is younger than Eocene. Our data show that a zone of high strain associated with strike-slip motion extends from Caleta Olla to Bahía Pia where it connects to the zone of normal faulting. Along with another high-strain strike-slip system at Seno Ventisquero, this zone of strike-slip faulting forms a ~10 km wide left step over centered on the normal faults at Bahía Pia and Seno Cerrado. The transtensional step over explains the concentration of horizontal stretching lineations and steep foliation planes along the shores of the Beagle Channel, including in the Yamana and Timbales regions described by *Cunningham* [1995], and the presence of late normal faulting first described by *Dalziel and Brown* [1989]. Similar step overs occur in the eastern part of Tierra del Fuego [*Menichetti et al.*, 2008].

7. Conclusions

[62] Detrital zircon ages from sedimentary rocks that filled the Rocas Verdes basin indicate that Upper Jurassic igneous rocks were a significant source of detritus into the rift. Ages at ~148 Ma provides a maximum depositional age for the sediment. This age, which matches those obtained from the northern part of the basin, suggests that the basin opened approximately simultaneously along its length.

[63] Imbricated, northeast vergent thrusts that placed basaltic crust of the Rocas Verdes basin floor on continental crust define the leading edge of the obducted Rocas Verdes terrane in Cordillera Darwin. U-Pb zircon crystallization ages show that basin inversion and collapse began and obduction occurred prior to ~86 Ma. A > 1 km thick ductile thrust that was coeval with moderate high pressure, upper amphibolite facies metamorphism supports interpretations that a part of the basaltic floor of the Rocas Verdes basin and adjacent continental crust were underthrust to the southwest beneath a volcanic arc during this period and fueled arc magmatism. The underthrusting of first basaltic crust and then continental crust as the basin

closed appears to have caused the obduction. During this early stage of basin inversion, obduction-related thrusts formed a narrow (~60 km wide) asymmetric wedge that persisted for tens of millions of years until a subsequent phase of mostly Paleogene out-of-sequence thrusting internally thickened and expanded the wedge. This latter phase, which formed a bivergent orogen cored by the high-grade kyanite-bearing rocks of Cordillera Darwin, appears to have resulted from a back-arc collision between the Patagonian batholith and adjacent South American continental crust as the Rocas Verdes basin finally collapsed. At this stage back thrusts and back folds formed pop ups above larger northeast vergent thrusts in the hinterland of the orogen. A minimum of ~50 km of horizontal shortening (~70%) occurred within Cordillera Darwin during this phase. A lack of marker units precludes determination of shortening magnitudes during the previous obduction phase. Out-of-sequence thrusting and internal thickening resulted in the exhumation of both high-grade basement and Upper Jurassic igneous rocks in Cordillera Darwin, which were a significant source of detritus into the Magallanes foreland basin at this time. Following these events, the Magallanes fold-thrust belt propagated rapidly into the foreland, suggesting that this lateral growth occurred to maintain the taper of the thrust wedge, which was perturbed by out-of-sequence thrusting.

[64] Ductile and brittle strike-slip, oblique-slip, and normal faults of the Beagle Channel fault zone postdate all thrust-related structures. The highest strains occur within one kilometer of the Beagle Channel. Large (up to 4–5 km wide) grabens form part of this system. Normal faults at the mouth of Bahía Pia uplifted the high-grade rocks of Cordillera Darwin in their footwalls and form part of a ~10 km wide transtensional step over of probable Neogene age.

[65] **Acknowledgments.** Funding to support this work was provided by the National Science Foundation (EAR-0635940 to K.K.). We thank DIFROL (Dirección Nacional de Fronteras y Límites del Estado) and the Chilean Navy for permission to visit and sample localities along the Beagle Channel. We are greatly indebted to Javier Álvarez and Fernando Poblete, geology students from the Universidad de Chile, who were excellent in the field. We thank M. Calderón for numerous helpful discussions and C. Gerbi and D. Barbeau for thorough reviews. J. Vargas completed the mineral separations at the University of Chile. We thank Captain Charles Porter for a cruise on *Ocean Tramp*, captains Keri Pashuk and Greg Landreth on *Northanger*, and Captain Edwin Olivares on *Patriota*.

References

Alabaster, T., and B. C. Storey (1990), Modified Gulf of California model for south Georgia, north Scotia Ridge, and implications for the Rocas Verdes back arc basin, southern Andes, *Geology*, *18*, 497–500, doi:10.1130/0091-7613(1990)018<0497:MGOCMF>2.3.CO;2.

Allen, R. B. (1982), Geología de la Cordillera Sarmiento, Andes Patagónicos, entre los 51°00′ y 52°15′ Lat. S, Magallanes, Chile, *Bull. 38*, 46 pp., Serv. Nac. de Geol. y Miner.-Chile, Santiago, Chile.

Allmendinger, R. W., T. E. Jordan, S. M. Kay, and B. L. Isacks (1997), The evolution of the Altiplano-Puna plateau of the central Andes, *Annu. Rev. Earth Planet. Sci.*, *25*, 139–174, doi:10.1146/annurev.earth.25.1.139.

Álvarez, J. (2007), Evolución geodinámica del Complejo Metamórfico Cordillera Darwin, Tierra del Fuego, XII Región, Chile, thesis, 79 pp., Univ. de Chile, Santiago. April.

Alvarez-Marrón, J., K. R. McClay, S. Harambour, L. Rojas, and J. Skarmeta (1993), Geometry and evolution of the frontal part of the Magallanes foreland thrust and fold belt (Vicuña Area), Tierra del Fuego, southern Chile, *AAPG Bull.*, *77*, 1904–1921.

Barbeau, D. L., E. B. Olivero, N. L. Swanson-Hysell, K. M. Zahid, K. E. Murray, and G. E. Gehrels (2009), Detrital-zircon geochronology of the eastern Magallanes foreland basin: Implications for Eocene kinematics of the northern Scotia Arc and Drake Passage, *Earth Planet. Sci. Lett.*, *284*(3–4), 489–503, doi:10.1016/j.epsl.2009.05.014.

Beck, S. L., and G. Zandt (2002), The nature of orogenic crust in the central Andes, *J. Geophys. Res.*, *107* (B10), 2230, doi:10.1029/2000JB000124.

Biddle, K. T., M. A. Uliana, R. M. Mitchum Jr., M. G. Fitzgerald, and R. C. Wright (1986), The stratigraphic and structural evolution of the central and eastern Magallanes basin, southern South America, *Spec. Publ. Int. Assoc. Sedimentol.*, *8*, 41–61.

Bruhn, R., C. Stern, and M. de Wit (1978), Field and geochemical data bearing on the development of a Mesozoic volcano-tectonic rift zone and back-arc basin in southernmost South America, *Earth Planet. Sci. Lett.*, *41*, 32–46, doi:10.1016/0012-821X(78)90039-0.

Calderón, M., A. Fildani, F. Hervé, C. M. Fanning, A. Weislogel, and U. Cordani (2007), Late Jurassic bimodal magmatism in the northern sea-floor remnant of the Rocas Verdes basin, southern Patagonian Andes, *J. Geol. Soc.*, *164*, 1011–1022, doi:10.1144/0016-76492006-102.

Cunningham, W. D. (1993), Strike-slip faults in the southernmost Andes and the development of the Patagonian orocline, *Tectonics*, *12*(1), 169–186, doi:10.1029/92TC01790.

Cunningham, W. D. (1994), Uplifted ophiolitic rocks on Isla Gordon, southernmost Chile: Implications for the closure history of the Rocas Verdes marginal basin and the tectonic evolution of the Beagle Channel region, *J. South Am. Earth Sci.*, *7*, 135–147, doi:10.1016/0895-9811(94)90004-3.

Cunningham, W. D. (1995), Orogenesis at the southern tip of the Americas: The structural evolution of the Cordillera Darwin Metamorphic Complex, southernmost Chile, *Tectonophysics*, *244*, 197–229, doi:10.1016/0040-1951(94)00248-8.

Dahlen, F. A. (1990), Critical taper model of fold-and-thrust belts and accretionary wedges, *Annu. Rev. Earth Planet. Sci.*, *18*, 55–99, doi:10.1146/annurev.ea.18.050190.000415.

Dahlstrom, C. D. A. (1969), Balanced cross-sections, *Can. J. Earth Sci.*, *6*, 743–757.

Dalziel, I. W. D. (1981), Back-arc extension in the southern Andes: A review and critical reappraisal, *Philos. Trans. R. Soc. London, Ser. A*, *300*, 319–335, doi:10.1098/rsta.1981.0067.

Dalziel, I. W. D. (1982), Pre-Jurassic history of the Scotia Arc region, in *Antarctic Geoscience*, edited by C. Craddock, pp. 111–126, Univ. of Wis. Press, Madison.

Dalziel, I. W. D. (1986), Collision and Cordilleran orogenesis, in *Collision Tectonics*, edited by M. P. Coward and A. C. Ries, *Geol. Soc. Spec. Publ.*, *19*, 380–404.

Dalziel, I. W. D., and R. L. Brown (1989), Tectonic denudation of the Cordillera Darwin metamorphic core complex, Tierra del Fuego: Implications for cordilleran orogenesis, *Geology*, *17*, 699–703, doi:10.1130/0091-7613(1989)017<0699:TDOTDM>2.3.CO;2.

Dalziel, I. W. D., and D. H. Elliot (1971), Evolution of the Scotia Arc, *Nature*, *233*, 246–252, doi:10.1038/233246a0.

Dalziel, I. W. D., and D. H. Elliot (1973), The Scotia Arc and Antarctic Margin, in *The Ocean Basins and Margins*, vol. 1, *The South Atlantic*, edited by A. E. M. Nairn and F. G. Stehli, pp. 171–245, Plenum, New York.

Dalziel, I. W. D., M. F. deWit, and K. F. Palmer (1974), Fossil marginal basin in the southern Andes, *Nature*, *250*, 291–294, doi:10.1038/250291a0.

Darwin, C. R. (1846), *Geological Observations on South America. Being the Third Part of the Geology of the Voyage of the Beagle, Under the Command of Capt. FitzRoy, R.N. During the Years 1832 to 1836*, 279 pp., Smith Elder, London.

Davis, D., J. Suppe, and F. A. Dahlen (1983), Mechanics of fold-and-thrust belts and accretionary wedges, *J. Geophys. Res.*, *88*, 1153–1172, doi:10.1029/JB088iB02p01153.

Diraison, M., P. R. Cobbold, D. Gapais, A. R. Rossello, and C. Le Corre (2000), Cenozoic crustal thickening, wrenching and rifting in the foothills of the southernmost Andes, *Tectonophysics*, *316*, 91–119, doi:10.1016/S0040-1951(99)00255-3.

Dott, R. H., Jr., R. D. Winn Jr., M. J. de Wit, and R. L. Bruhn (1977), Tectonic and sedimentary significance of Cretaceous Tekenika Beds of Tierra del Fuego, *Nature*, *266*, 620–622, doi:10.1038/266620a0.

Dott, R. H., Jr., R. D. Winn Jr., and C. H. L. Smith (1982), Relationship of Late Mesozoic and Early Cenozoic sedimentation to the tectonic evolution of the southernmost Andes and Scotia Arc, in *Antarctic Geoscience*, edited by C. Craddock, pp. 193–201, Univ. of Wis. Press, Madison.

Elliott, D. (1983), The construction of balanced cross-sections, *J. Struct. Geol.*, *5*, 101, doi:10.1016/0191-8141(83)90035-4.

Fildani, A., and A. M. Hessler (2005), Stratigraphic record across a retroarc basin inversion: Rocas Verdes-Magallanes basin, Patagonian Andes, Chile, *Geol. Soc. Am. Bull.*, *117*, 1596–1614, doi:10.1130/B25708.1.

Fildani, A., T. D. Cope, S. A. Graham, and J. L. Wooden (2003), Initiation of the Magallanes foreland basin:

Timing of the southernmost Patagonian Andes orogeny revised by detrital-zircon provenance analysis, *Geology*, *31*, 1081–1084, doi:10.1130/G20016.1.

Ghiglione, M. C., and V. A. Ramos (2005), Progression of deformation and sedimentation in the southernmost Andes, *Tectonophysics*, *405*, 25–46, doi:10.1016/j.tecto.2005.05.004.

Gombosi, D. J., D. L. Barbeau Jr., and J. I. Garver (2009), New thermochronometric constraints on the rapid Palaeogene exhumation of the Cordillera Darwin complex and related thrust sheets in the Fuegian Andes, *Terra Nova*, *21*, 507–515, doi:10.1111/j.1365-3121.2009.00908.x.

Gust, D. A., K. T. Biddle, D. W. Phelps, and M. A. Uliana (1985), Associated Middle to Late Jurassic volcanism and extension in southern South America, *Tectonophysics*, *116*, 223–253, doi:10.1016/0040-1951(85)90210-0.

Halpern, M. (1973), Regional geochronology of Chile south of 50° latitude, *Geol. Soc. Am. Bull. 84*, 2407–2422, doi:10.1130/0016-7606(1973)84<2407:RGOCSO>2.0.CO;2.

Halpern, M., and D. C. Rex (1972), Time of folding of the Yahgan Formation and age of the Tekenika Beds, southern Chile, South America, *Geol. Soc. Am. Bull.*, *83*, 1881–1886, doi:10.1130/0016-7606(1972)83[1881:TOFOTY]2.0.CO;2.

Hanson, R. E., and T. J. Wilson (1991), Submarine rhyolitic volcanism in a Jurassic proto-marginal basin, southern Andes, Chile and Argentina, in *Andean Magmatism and Its Tectonic Setting*, edited by R. S. Harmon and C. Rapela, *Spec. Pap. Geol. Soc. Am.*, *265*, 13–27.

Hervé, F., and C. Mpodozis (2005), The western Patagonia terrane collage: New facts and some thought-provoking possibilities, in *Gondwana 12, Geological and Biological Heritage of Gondwana*, edited by R. J. Pankhurst and G. D. Veiga, p. 196, Acad. Nac. de Cienc., Córdoba, Argentina.

Hervé, F., E. Nelson, K. Kawashita, and M. Suárez (1981), New isotopic ages and the timing of orogenic events in the Cordillera Darwin, southernmost Chilean Andes, *Earth Planet. Sci. Lett.*, *55*, 257–265, doi:10.1016/0012-821X(81)90105-9.

Hervé, M., M. Suárez, and A. Puig (1984), The Patagonian batholith S of Tierra del Fuego, Chile: Timing and tectonic implications, *J. Geol. Soc.*, *141*, 909–917, doi:10.1144/gsjgs.141.5.0909.

Hervé, F., R. J. Pankhurst, C. M. Fanning, M. Calderón, and G. M. Yaxley (2007), The South Patagonian batholith: 150 My of granite magmatism on a plate margin, *Lithos*, *97*, 373–394, doi:10.1016/j.lithos.2007.01.007.

Hervé, F., M. Fanning, R. J. Pankhurst, C. Mpodozis, K. Klepeis, M. Calderón, and S. Thomson (2010), Detrital zircon SHRIMP U-Pb age study of the Cordillera Darwin Metamorphic Complex: Sedimentary sources and implications for the evolution of the Pacific margin of Gondwana, *J. Geol. Soc.*, *167*, 555–568, doi:10.1144/0016-76492009-124.

Hubbard, S. M., B. W. Romans, and S. A. Graham (2008), Deep-water foreland basin deposits of the Cerro Toro Formation, Magallanes basin, Chile: Architectural elements of a sinuous basin axial channel belt, *Sedimentology*, *55*, 1333–1359, doi:10.1111/j.1365-3091.2007.00948.x.

Jokat, W., T. Boebel, M. König, and U. Meyer (2003), Timing and geometry of early Gondwana breakup, *J. Geophys. Res.*, *108*(B9), 2428, doi:10.1029/2002JB001802.

Katz, H. R. (1963), Revision of Cretaceous stratigraphy in Patagonian Cordillera of Ultima Esperanza, Magallanes Province, Chile, *AAPG Bull.*, *47*, 506–524.

Katz, H. R. (1973), Contrasts in tectonic evolution of orogenic belts in the southwest Pacific, *J. R. Soc. N. Z.*, *3*, 333–362.

Klepeis, K. A. (1994a), Relationship between uplift of the metamorphic core of the southernmost Andes and shortening in the Magallanes foreland fold and thrust belt, Tierra Del Fuego, Chile, *Tectonics*, *13*, 882–904, doi:10.1029/94TC00628.

Klepeis, K. A. (1994b), The Magallanes and Deseado fault zones: Major segments of the South American-Scotia transform plate boundary in southernmost South America, Tierra del Fuego, *J. Geophys. Res.*, *99*(B11), 22,001–22,014, doi:10.1029/94JB01749.

Klepeis, K. A., and J. A. Austin (1997), Contrasting styles of superposed deformation in the southernmost Andes, *Tectonics*, *16*(5), 755–776, doi:10.1029/97TC01611.

Kley, J., C. R. Monaldi, and J. A. Salfity (1999), Along-strike segmentation of the Andean foreland: Causes and consequences, *Tectonophysics*, *301*, 75–94, doi:10.1016/S0040-1951(98)90223-2.

Kohn, M. J., F. S. Spear, and I. W. D. Dalziel (1993), Metamorphic P-T paths from Cordillera Darwin, a core complex in Tierra del Fuego, Chile, *J. Petrol.*, *34*(3), 519–542.

Kohn, M. J., F. S. Spear, T. M. Harrison, and I. W. D. Dalziel (1995), $^{40}Ar/^{39}Ar$ geochronology and P-T-t paths from the Cordillera Darwin metamorphic complex, Tierra del Fuego, Chile, *J. Metamorph. Geol.*, *13*, 251–270, doi:10.1111/j.1525-1314.1995.tb00217.x.

Kraemer, P. E. (2003), Orogenic shortening and the origin of the Patagonian orocline, 56°S, *J. South Am. Earth Sci.*, *15*, 731–748, doi:10.1016/S0895-9811(02)00132-3.

Kranck, E. H. (1932), Geological investigations in the Cordillera of Tierra del Fuego, *Acta Geogr. Soc. Geogr. Fenniae*, *4*(2), 1–231.

Lodolo, E., M. Menichetti, R. Bartole, Z. Ben Avram, A. Tassone, and H. Lippai (2003), Magallanes-Fagnano continental transform fault (Tierra del Fuego, southernmost South America), *Tectonics*, *22*(6), 1076, doi:10.1029/2003TC001500.

Ludwig, K. R. (2001), SQUID 1.02: A user's manual, *Spec. Publ. 2*, Berkeley Geochronol. Cent., Berkeley, Calif.

Marrett, R. A., and R. W. Allmendinger (1990), Kinematic analysis of fault-slip data, *J. Struct. Geol.*, *12*(8), 973–986, doi:10.1016/0191-8141(90)90093-E.

Marshak, S., and G. Mitra (1988), *Basic Methods of Structural Geology*, 446 pp., Prentice Hall, Englewood Cliffs, N. J.

Menichetti, M., E. Lodolo, and A. Tassone (2008), Structural geology of the Fueguian Andes and Magallanes fold-and-thrust belt-Tierra del Fuego Island, *Geol. Acta*, *6*(1), 19–42.

Mpodozis, C., and R. W. Allmendinger (1993), Extensional tectonics, Cretaceous Andes, northern Chile (27°S), *Geol. Soc. Am. Bull.*, *105*, 1462–1477, doi:10.1130/0016-7606(1993)105<1462:ETCANC>2.3.CO;2.

Mpodozis, C., and L. Rojas (2006), Orogénesis en los Andes Patagónicos Australes de Tierra del Fuego: Cierre de una "Cuenca Marginal" o Colisión Intracontinental?, paper presented at XI Congreso Geológico Chileno, Antofagasta, Chile, 7–11 Aug.

Natland, M. L., E. Gonzalez, A. Cañon, and M. Ernst (1974), A system of stages for correlation of Magallanes basin sediments, *Mem. Geol. Soc. Am.*, *139*, 126 pp.

Nelson, E. P. (1982), Post-tectonic uplift of the Cordillera Darwin orogenic core complex: Evidence from fission track geochronology and closing temperature-time relationship, *J. Geol. Soc.*, *139*, 755–761, doi:10.1144/gsjgs.139.6.0755.

Nelson, E. P., I. W. D. Dalziel, and A. G. Milnes (1980), Structural geology of the Cordillera Darwin-collision style orogenesis in the southernmost Andes, *Eclogae Geol. Helv.*, *73*, 727–751.

Olivero, E. B., and N. Malumián (2008), Mesozoic-Cenozoic stratigraphy of the Fuegian Andes, Argentina, *Geol. Acta*, *6*(1), 15–18.

Olivero, E. B., and D. R. Martinioni (2001), A review of the geology of the Argentinean Fuegian Andes, *J. South Am. Earth Sci.*, *14*, 175–188, doi:10.1016/S0895-9811(01)00016-5.

Ortiz, M. (2007), Condiciones de formación del Complejo Metamórfico Cordillera Darwin, al Sur de Seno Almirantazgo, Region de Magallanes, Chile, thesis, 79 pp., Univ. de Chile, Santiago, Chile, April.

Pankhurst, R. J., T. R. Riley, C. M. Fanning, and S. Kelley (2000), Episodic silicic volcanism in Patagonia and the Antarctic Peninsula: Chronology of magmatism associated with the break-up of Gondwana, *J. Petrol.*, *41*, 605–625, doi:10.1093/petrology/41.5.605.

Pankhurst, R. J., C. W. Rapela, W. P. Loske, M. Marquez, and C. M. Fanning (2003), Chronological study of the pre-Permian basement rocks of southern Patagonia, *J. South Am. Earth Sci.*, *16*, 27–44, doi:10.1016/S0895-9811(03)00017-8.

Ramsey, J. G. (1967), *Folding and fracturing of rocks*, 568 pp., McGraw-Hill, New York.

Rojas, L., and C. Mpodozis (2006), Geología Estructural de la Faja Plegada y Corrida del sector chileno de Tierra del Fuego, Andes Patagónicos australes, paper presented at XI Congreso Geológico Chileno, Antofagasta, Chile, 7–11 Aug.

Romans, B. W., A. Fildani, S. A. Graham, S. M. Hubbard, and J. A. Covault (2010), Importance of predecessor basin history on sedimentary fill of a retroarc foreland basin: Provenance analysis of the Cretaceous Magallanes basin, Chile (50°S–52°S), *Basin Res.*, doi:10.1111/j.1365-2117.2009.00443.x, in press.

Rossello, E. A. (2005), Kinematics of the Andean sinistral wrenching along the Fagnano-Magallanes fault zone (Argentina-Chile Fuegian Foothills), paper presented at 6th International Symposium on Andean Geodynamics, Inst. de Rech. pour le Dév., Barcelona, Spain.

SERNAGEOMIN (2002), Mapa geológico de Chile, *Carta Geol. Chile, Ser. Geol. Básica 75*, 1 map and 3 sheets, scale 1:1,000,000.

Sobolev, S. V., and A. Y. Babeyko (2005), What drives orogeny in the Andes?, *Geology*, *33*, 617–620, doi:10.1130/G21557AR.1.

Stern, C. R. (1980), Geochemistry of Chilean ophiolites: Evidence of the compositional evolution of the mantle source of back-arc basin basalts, *J. Geophys. Res.*, *85*, 955–966, doi:10.1029/JB085iB02p00955.

Stern, C. R., and M. J. de Wit (2003), Rocas Verdes ophiolites, southernmost South America: Remnants of progressive stages of development on oceanic-type crust in a continental margin back-arc basin, in *Ophiolites in Earth History*, edited by Y. Dilek and P. T. Robinson, *Geol. Soc. Spec. Publ.*, *218*, 665–683, doi:10.1144/GSL.SP.2003.218.01.32.

Stern, T., D. Okaya, and M. Scherwath (2002), Structure and strength of a continental transform from onshore-offshore seismic profiling of the South Island, New Zealand, *Earth Planets Space*, *54*, 1011–1019.

Suárez, M., and T. H. Pettigrew (1976), An upper Mesozoic island-arc-backarc system in the southern Andes and South Georgia, *Geol. Mag.*, *113*, 305–328, doi:10.1017/S0016756800047592.

Suárez, M., A. Puig, and M. Hervé (1985), Hoja Isla Hoste e islas adyacentes, XII Región, *Carta Geol. Chile, 65*, scale 1:250,000, 113 pp.

Tera, F., and G. J. Wasserburg (1972), U-Th-Pb systematics of three Apollo14 basalts and the problem of initial Pb in lunar rocks, *Earth Planet. Sci. Lett.*, *14*, 281–304, doi:10.1016/0012-821X(72)90128-8.

Tilmann, F., et al. (2003), Seismic imaging of the downwelling Indian lithosphere beneath central Tibet, *Science*, *300*, 1424–1427, doi:10.1126/science.1082777.

Torres Carbonell, P., L. Dimieri, and E. Olivero (2010), Progressive deformation of a Coulomb thrust-wedge: The eastern Fuegian Andes thrust-fold belt, in *Kinematic Evolution and Structural Styles of Fold-and-Thrust Belts*, edited by J. Poblet and R. Lisle, *Geol. Soc. Spec. Publ.*, in press.

Williams, I. S. (1998), U-Th-Pb geochronology by Ion Microprobe, in *Applications of Microanalytical*

Techniques to Understanding Mineralizing Processes, *Rev. Econ. Geol.*, vol. 7, edited by M. A. McKibben, W. C. Shanks III, and W. I. Ridley, pp. 1–35, Soc. of Econ. Geol., Littleton, Colo.

Wilson, T. J. (1983), Stratigraphic and structural evolution of the Ultima Esperanza foreland fold-thrust belt, Patagonian Andes, southern Chile, Ph.D. dissertation, Columbia Univ., New York.

Wilson, T. J. (1991), Transition from back-arc to foreland basin development in the southernmost Andes: Stratigraphic record from the Ultima Esperanza District, Chile, *Geol. Soc. Am. Bull. 103*, 98–111, doi:10.1130/0016-7606(1991)103<0098:TFBATF>2.3.CO;2.

P. Betka, Jackson School of Geosciences, University of Texas at Austin, Austin, TX 78722, USA.

G. Clarke, School of Geosciences, F09, University of Sydney, NSW 2006, Australia.

M. Fanning, Research School of Earth Sciences, Australian National University, Bldg. 61, Mills Rd., Acton 0200, Canberra, ACT, Australia.

F. Hervé, Departamento de Geología, Universidad de Chile, Casilla 13518, Correo 21, Santiago, Chile.

K. Klepeis, Department of Geology, University of Vermont, 180 Colchester Ave., Burlington, VT, 05405-0122, USA.

C. Mpodozis, Antofagasta Minerals, Apoquindo 4001, Piso 18, Santiago, Chile.

L. Rojas, Enap-Sipetrol, Av. Vitacura 2736, Piso 10, Las Condes, Santiago, Chile.

S. Thomson, Department of Geosciences, University of Arizona, 1040 E. 4th St., Tucson, AZ 85721-0077, USA.